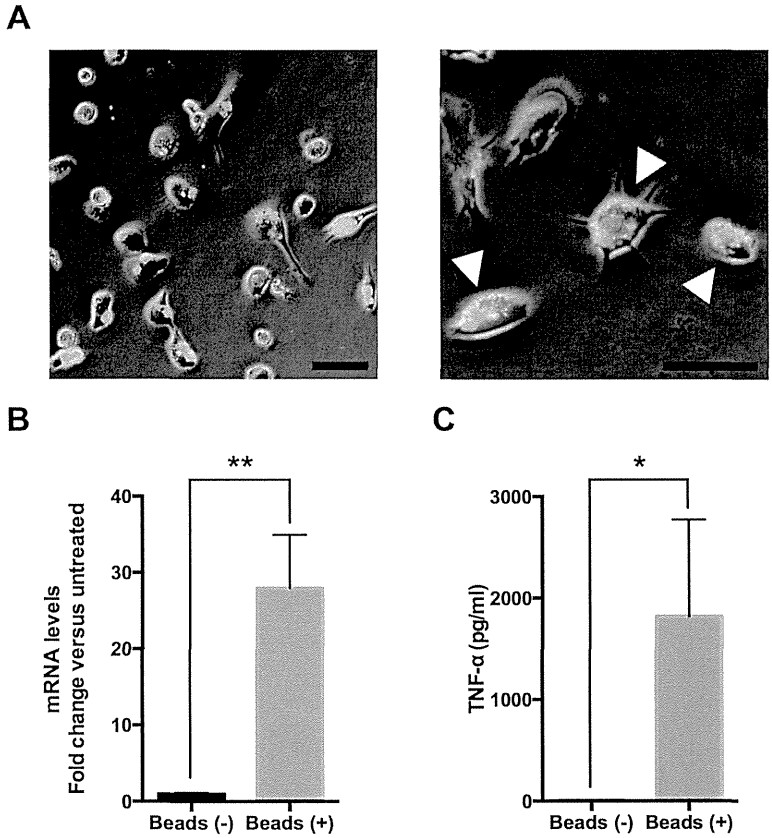

Figure 3 | Dynamic functional analysis of the iMG cells. (A) The iMG cells were incubated with FITC-conjugated latex beads for 24 hours, and phagocytic activity was observed by fluorescent microscopy. The iMG cells showed the ability of phagocytosis with morphological changes into an ameboid form (arrow head). Scale bar, 50 μm. (B and C) The ability of TNF-α production during phagocytosis was measured on the iMG cells. The iMG cells were incubated with latex beads for 72 hours. The extracted RNA and culture supernatant were analyzed by qRT-PCR and Cytometric Beads Array System (CBA), respectively. The mRNA expression (B) and protein level of TNF-α (C) on the iMG cells were significantly higher compared to controls (B, n = 4; C, n = 6). $*P < 0.05$, $**P < 0.01$. Error bars, SEM.

Especially, IL-34 has recently come to be known as a key molecule for the proliferation of microglia[32]. The present data have suggested that both GM-CSF and IL-34 from astrocytes are the minimum essential inducing-factors for microglia-like cells from hematopoietic cells.

The present results indicate that the iMG cells from a patient of NHD show slower (24 h) but not weaker (72 h) pro-inflammatory cytokines' responses compared to those from the healthy control, possibly due to the deletion of DAP12. In addition, suppression of IL-10 production from the iMG cells from the NHD patient indicates that human brain microglia of NHD patients tend to be shifted to pro-inflammatory reactions compared to those of healthy controls. Furthermore, the situation observed in the iMG cells from a NHD patient was replicated with iMG cells from a healthy control using siRNA. These data have suggested that DAP12 expression is a key factor in from the perspective of microglial immunoresponse such as cytokine production in NHD patients. In the present study, we examined the iMG cells from a female patient of NHD. Recent studies have suggested microglial functional differences between sexes[33]. Further investigations should focus on sex differences related to microglial dysfunction of NHD. DAP12 and TREM2 are the responsible genes of NHD, which mediate various important roles such as phagocytosis and cytokine production in osteoclasts, macrophages, dendritic cells and microglia[34]. A rodent study showed that deletion of DAP12 induces synaptic impairments due to microglial dysfunction[15]. Hamerman et al.[35] demonstrated that macrophage from DAP12-deficient mice increase inflammatory cytokines' responses, which suggest that DAP12-deleted microglia increase similar inflammatory response. These previous reports and our present findings based on the iMG cells from a NHD patient suggest that human NHD microglia has the potential to induce stronger and long-acting pro-inflammatory reactions compared to those of healthy human subjects.

In sum, we have shown a novel technique of developing directly induced microglia-like cells, named "iMG cells", with a combination of GM-CSF and IL-34 from adult human monocytes, easily and quickly without any virus, feeder cells, and genetic engineering. The iMG cells proved to have many characterizations of microglial cells, such as expressing $CD11b^{high}/CD45^{low}$ and $CX3CR1^{high}/CCR2^{low}$. Moreover, the iMG cells expressed dynamic functions such as phagocytosis and releasing pro- and anti- inflammatory cytokines. Further investigations such as microarray analysis should be conducted to validate the closeness of iMG cells to human primary microglial cells in the brain. Finally, we presented the translational utilities of the iMG cells for analyzing the underlying microglial pathophysiology of NHD. We believe that this novel technique will shed new light on solving unknown dynamic aspects of human microglial cells in various brain disorders.

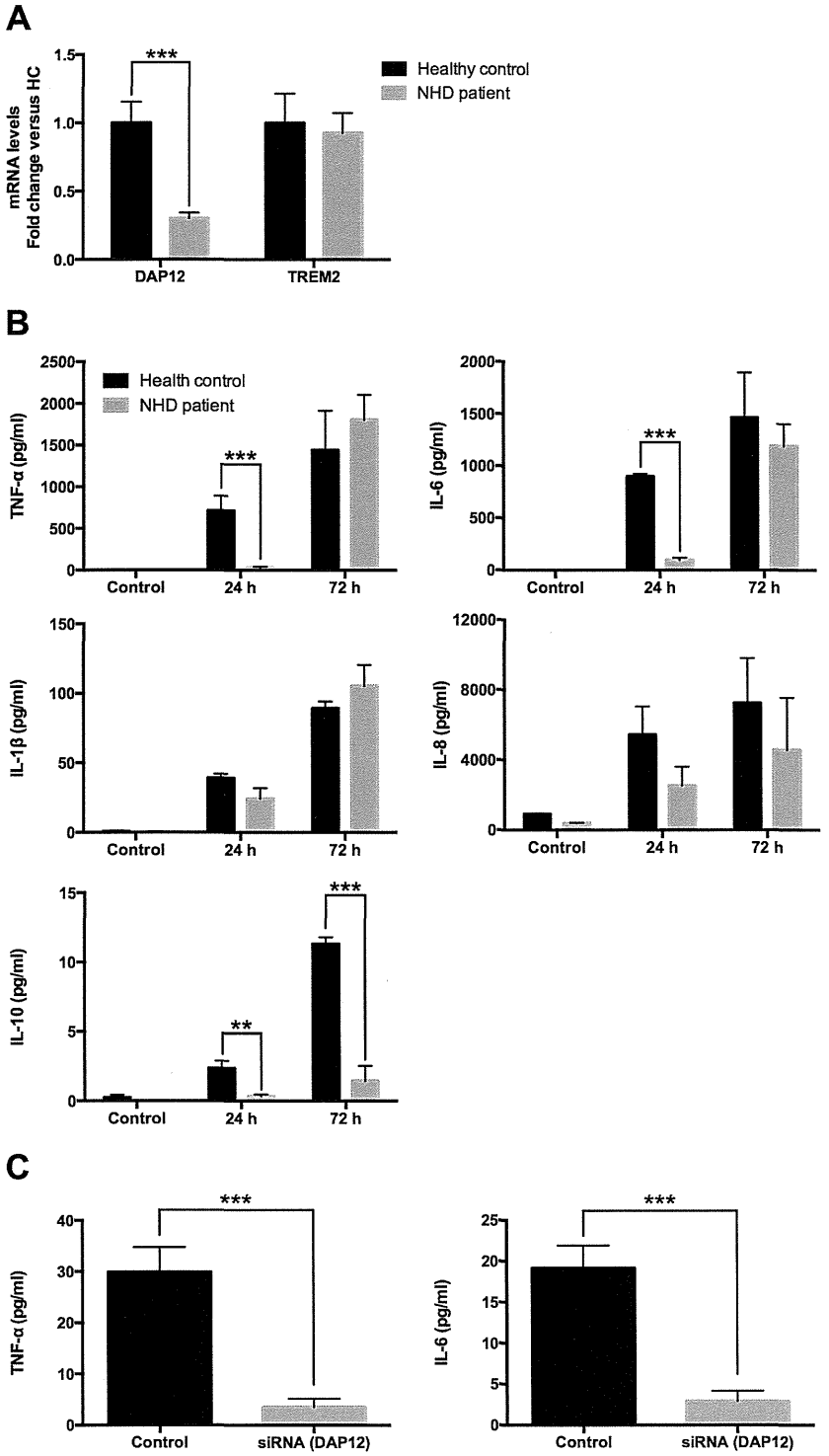

Figure 4 | Dynamic functional analysis of the iMG cells from a patient of NHD. (A) The iMG cells from the NHD patient showed significantly lower gene expression of DAP12 compared to those from the healthy control (n = 6). (B) Cytokine production from the iMG cells were compared between the NHD patient and the healthy control. The iMG cells from the NHD patient and the healthy control were incubated with latex beads for 24 or 72 hours, and culture supernatants were analyzed by CBA. In the iMG cells from the NHD patient, the production of pro-inflammatory cytokines (TNF-α and IL-6) was delayed, and that of anti-inflammatory cytokine (IL-10) was decreased (n = 4). (C) The effects of DAP12 silencing on the proinflammatory cytokine production. The iMG cells treated with siRNA were incubated with latex beads for 24 hours, and culture supernatants were analyzed by CBA In the iMG cells treated with siRNA, the production of pro-inflammatory cytokines was delayed (n = 8) $^{**}P < 0.01$, $^{***}P < 0.001$. Error bars, SEM.

Methods

Subjects. The present study was conducted in accordance with the World Medical Association's Declaration of Helsinki and was approved by the Ethics Committee of the Graduate School of Medical Sciences, Kyushu University and Osaka University. We recruited a middle-aged female patient, who was diagnosed with Nasu-Hakola disease (141delG in DAP12 gene) in her thirties. Based on informed consents both from the patient and a family member, we took a blood sample. Healthy adult volunteers including an age-matched female were also recruited.

Induction of induced microglia-like (iMG) cells from human peripheral blood. Peripheral blood was collected using a heparinized tube from healthy adult volunteers and a patient of NHD. Peripheral blood mononuclear cells (PBMC) were isolated by Histopaque-1077 (Sigma Chemical Co., St. Louis, MO) density gradient centrifugation. PBMC were resuspended with RPMI-1640 (Nacalai Tesque, Kyoto, Japan), 10% heat-inactivated fetal bovine serum (FBS; Endotoxin = 0.692 EU/ml; Japan Bio Serum, Hiroshima, Japan) and 1% antibiotics/antimycotic (Invitrogen, Carlsbad, CA). PBMC were plated onto culture chambers at a density of 4×10^5 cells/ml and cultured overnight in standard culture conditions (37°C, 5% CO_2). After overnight incubation, culture supernatant and non-adherent cells were removed. The adherent cells (monocytes) were cultured with RPMI-1640 Glutamax (Invitrogen) supplemented with 1% antibiotics/antimycotic and a mixture of the following candidate cytokines; recombinant human GM-CSF (10 ng/ml; R&D Systems, Minneapolis, MN), recombinant human IL-34 (100 ng/ml; R&D Systems) and M-CSF (10 ng/ml; Peprotec, Rocky Hill, NJ) in order to develop iMG cells. We also developed induced macrophage from human monocytes; monocytes were cultured with RPMI-1640 Glutamax supplemented with 1% antibiotics/antimycotic and recombinant human GM-CSF (10 ng/ml). All cells were cultured in standard culture conditions for up to 14 days.

Cell morphology. Morphological changes of cytokines-treated cells were examined using phase-contrast microscopy (TS100-F; Nikon Instech, Tokyo, Japan). Images were taken with a DS-Vi1 digital camera (Nikon Instech) and a DS-L3 control unit (Nikon Instech).

Flow cytometry. Flow cytometry was performed using a FACS Aria (BD Biosciences, Bedford, MA) with FACS Diva software (BD Biosciences). Flow cytometry data were analyzed using FlowJo software (Tree Star, San Carios, CA). For iMG phenotyping, fluorochrome conjugated monoclonal antibodies specific for human CD11b (APC-Vio770; Miltenyi Biotec, Gladbach, Germany), CD14 (FITC; Sigma), CD45 (PE; Miltenyi Biotec) and CD200R (Alexa647; Serotec, Oxford, UK) were used. Induced macrophage and iMG cells were cultured in 6-well plates (Corning, NY) at a density of 4×10^5 cells/ml. Cells were harvested by non-enzymatic cell dissociation solution (Sigma) and cell lifter (Corning). The cells were washed with MACS buffer (Miltenyi Biotec) and incubated for 5 minutes at 4°C in FcR-blocking reagent (Miltenyi Biotec). Antibodies were incubated with cell suspension for 30 minutes at 4°C, washed with calcium-magnesium-free phosphate-buffered saline (PBS(-)), resuspended and fixed with 1% paraformaldehyde (Wako, Osaka, Japan) in PBS(-). The fluorescence intensity of the cells was measured.

Indirect immunofluorescence for flow cytometry was performed using the following antibodies: rabbit anti-CX3CR1 antibody (Immuno-Biological Laboratories, Gunma, Japan) and mouse anti-CCR2 antibody (R&D Systems). The monocytes and iMG cells were treated with the same process until the primary antibody staining. After primary staining, washed with MACS buffer and were stained with Alexa488- or Alexa546-conjugated secondary antibodies (Invitrogen). The ratio of CX3CR1 to CCR2 was calculated by the fluorescent intensity of each fluorochrome.

Immunocytochemistry. In immunocytochemistry, iMG cells and monocytes were cultured in 8-well chambers (LabTec chamber slide system; Nalge Nunc International, Rochester, NY) at a density of 4×10^5 cells/ml. These cells were fixed with 4% paraformaldehyde (Wako) for 20 minutes and then rinsed thrice with PBS(-) for 5 minutes. Indirect immunofluorescence was performed using the following antibodies: rabbit anti-CX3CR1 antibody (1 : 500 dilution; Immuno-Biological Laboratories, Gunma, Japan) and mouse anti-CCR2 antibody (1 : 500 dilution; R&D Systems). Cells were incubated in primary antibodies diluted in 0.1% Triton-X 100 in PBS containing 5% normal goat serum at 4°C overnight. After rinsing thrice with PBS(-) for 5 min, Alexa488- or Alexa546-conjugated secondary antibodies (Invitrogen) were used for detection. Fluorescent images were taken with a confocal laser scanning microscope (LSM-780; Carl Zeiss, Jena, Germany).

Quantitative real time-polymerase chain reaction (qRT-PCR). To assess the gene expression patterns in iMG cells after the treatment of IL-4, dexamethasone or during phagocytosis, we performed qRT-PCR using a LightCycler 480 system (Roche Diagnostics, Mannheim, Germany). IL-4 (40 ng/ml; Peprotec), dexamethasone (2 nM; Sigma) or latex beads-rabbit IgG-FITC solution (Cayman Chemical) was added to the iMG cells and incubated for 72 hours in standard culture conditions. After incubation, the iMG cells were washed and the total RNA was extracted using a High Pure RNA Isolation kit (Roche Diagnostics) according to the manufacturer's protocol, and subjected to cDNA synthesis using a Transcriptor First Strand cDNA Synthesis kit (Roche Diagnostics). qRT-PCR for HLA-DR, CD45, TNF-α, CCR7, CCL18 and CD200R was performed using each primer (Supplementary Table 1). Beta 2-microglobulin of Universal ProbeLibrary (Roche Diagnostics) was used as a house-keeping control gene. Fold changes were depicted in mRNA levels after stimulation compared with unstimulated cells.

Using the iMG cells from a female NHD patient and an age-sex matched healthy control, we examined the gene expression of DAP12 and TREM2 by qRT-PCR. The iMG cells were washed and the total RNA was extracted respectively, and qRT-PCR was performed using each primer (Supplementary Table 1). Beta 2-microglobulin was used as a house-keeping control gene. Fold changes were depicted in mRNA levels after stimulation compared with unstimulated cells.

Phagocytosis. Phagocytosis was examined by fluorescent microscopy using Phagocytosis Assay Kit (Cayman Chemical, Ann Arbor, MI) according to the manufacturer's protocol. The iMG cells were cultured in 8-well chambers (Nalge Nunc International) at a density of 4×10^5 cells/ml. We added 50 μl of the latex beads-rabbit IgG-FITC solution to each well of the chamber, and incubated the cells in standard culture conditions for 24 hours. After discarding the supernatant by careful aspiration, we quenched surface-bound fluorescence, added 125 μl of trypan blue solution to each well of the chamber, and incubated for two minutes at room temperature. Each well was analyzed by using a fluorescence microscope (Olympus IX-71, Tokyo, Japan) and DP71 digital camera system (Olympus).

Cytokine measurement. Secretion of pro- and anti- inflammatory cytokines (TNF-α, IL-1β, IL-6, IL-8 and IL-10) during phagocytosis was measured from culture supernatants using Cytometric Beads Array System (CBA; BD Biosciences) according to the manufacturer's protocol. Latex beads-rabbit IgG-FITC solution (Cayman Chemical) was added to the iMG cells and incubated for 24 or 72 hours in standard culture conditions. After incubation, culture supernatants were centrifuged at 10000 × g for 10 minutes and kept frozen at −80°C until assayed. The culture supernatants were incubated with the cytokine capture beads and PE-conjugated detection antibodies for 3 hours at room temperature. Afterwards, the capture beads were washed and measurement data were acquired using a FACS Canto™ flow cytometer (BD Biosciences). The data analysis was performed using FCAP Array software (BD Biosciences).

Gene silencing of DAP12. Gene silencing assay was performed using siRNA (DAP12; Santa Cruz, USA) and RNAiMAX (Invitrogen) according to the manufacturer's protocol. The mix solution of siRNA and RNAiMAX was added to the iMG cells. After overnight incubation, the medium was changed to the culture medium and incubated for 48 hours. The siRNA-modified iMG cells were used for cytokine assay.

Statistical analysis. Analysis of comparisons between groups were conducted by two-tailed Student's t-test.

1. Ginhoux, F. *et al.* Fate mapping analysis reveals that adult microglia derive from primitive macrophages. *Science* **330**, 841–845 (2010).
2. Nimmerjahn, A., Kirchhoff, F. & Helmchen, F. Resting microglial cells are highly dynamic surveillants of brain parenchyma in vivo. *Science* **308**, 1314–1318 (2005).
3. Kettenmann, H., Hanisch, U. K., Noda, M. & Verkhratsky, A. Physiology of microglia. *Physiol Rev* **91**, 461–553 (2011).
4. Ransohoff, R. M. & Perry, V. H. Microglial physiology: unique stimuli, specialized responses. *Annu Rev Immunol* **27**, 119–145 (2009).
5. Graeber, M. B. Changing face of microglia. *Science* **330**, 783–788 (2010).
6. Block, M. L., Zecca, L. & Hong, J. S. Microglia-mediated neurotoxicity: uncovering the molecular mechanisms. *Nat Rev Neurosci* **8**, 57–69 (2007).
7. Hanisch, U. K. & Kettenmann, H. Microglia: active sensor and versatile effector cells in the normal and pathologic brain. *Nat Neurosci* **10**, 1387–1394 (2007).
8. Kato, T. A. *et al.* Neurotransmitters, psychotropic drugs and microglia: clinical implications for psychiatry. *Curr Med Chem* **20**, 331–344 (2013).
9. Hakola, H. P. Neuropsychiatric and genetic aspects of a new hereditary disease characterized by progressive dementia and lipomembranous polycystic osteodysplasia. *Acta Psychiatr Scand Suppl* **232**, 1–173 (1972).
10. Nasu, T., Tsukahara, Y. & Terayama, K. A lipid metabolic disease-"membranous lipodystrophy"-an autopsy case demonstrating numerous peculiar membrane-structures composed of compound lipid in bone and bone marrow and various adipose tissues. *Acta Pathol Jpn* **23**, 539–558 (1973).
11. Kaneko, M., Sano, K., Nakayama, J. & Amano, N. Nasu-Hakola disease: The first case reported by Nasu and review. *Neuropathology* **30**, 463–470 (2010).
12. Paloneva, J. *et al.* CNS manifestations of Nasu-Hakola disease: a frontal dementia with bone cysts. *Neurology* **56**, 1552–1558 (2001).
13. Paloneva, J. *et al.* Loss-of-function mutations in TYROBP (DAP12) result in a presenile dementia with bone cysts. *Nat Genet* **25**, 357–361 (2000).
14. Paloneva, J. *et al.* Mutations in two genes encoding different subunits of a receptor signaling complex result in an identical disease phenotype. *Am J Hum Genet* **71**, 656–662 (2002).
15. Roumier, A. *et al.* Impaired synaptic function in the microglial KARAP/DAP12-deficient mouse. *J Neurosci* **24**, 11421–11428 (2004).
16. Satoh, J. *et al.* Immunohistochemical characterization of microglia in Nasu-Hakola disease brains. *Neuropathology* **31**, 363–375 (2011).
17. Mattis, V. B. & Svendsen, C. N. Induced pluripotent stem cells: a new revolution for clinical neurology? *Lancet Neurol* **10**, 383–394 (2011).
18. Dimos, J. T. *et al.* Induced pluripotent stem cells generated from patients with ALS can be differentiated into motor neurons. *Science* **321**, 1218–1221 (2008).

19. Pfisterer, U. *et al.* Direct conversion of human fibroblasts to dopaminergic neurons. *Proc Natl Acad Sci U S A* **108**, 10343–10348 (2011).
20. Qiang, L. *et al.* Directed conversion of Alzheimer's disease patient skin fibroblasts into functional neurons. *Cell* **146**, 359–371 (2011).
21. Pang, Z. P. *et al.* Induction of human neuronal cells by defined transcription factors. *Nature* **476**, 220–223 (2011).
22. Wang, Y. *et al.* IL-34 is a tissue-restricted ligand of CSF1R required for the development of Langerhans cells and microglia. *Nat Immunol* **13**, 753–760 (2012).
23. Aloisi, F., De Simone, R., Columba-Cabezas, S., Penna, G. & Adorini, L. Functional maturation of adult mouse resting microglia into an APC is promoted by granulocyte-macrophage colony-stimulating factor and interaction with Th1 cells. *J Immunol* **164**, 1705–1712 (2000).
24. Erblich, B., Zhu, L., Etgen, A. M., Dobrenis, K. & Pollard, J. W. Absence of colony stimulation factor-1 receptor results in loss of microglia, disrupted brain development and olfactory deficits. *PLoS One* **6**, e26317 (2011).
25. Nandi, S. *et al.* The CSF-1 receptor ligands IL-34 and CSF-1 exhibit distinct developmental brain expression patterns and regulate neural progenitor cell maintenance and maturation. *Dev Biol* **367**, 100–113 (2012).
26. Sedgwick, J. D. *et al.* Isolation and direct characterization of resident microglial cells from the normal and inflamed central nervous system. *Proc Natl Acad Sci U S A* **88**, 7438–7442 (1991).
27. Melief, J. *et al.* Phenotyping primary human microglia: tight regulation of LPS responsiveness. *Glia* **60**, 1506–1517 (2012).
28. Mizutani, M. *et al.* The fractalkine receptor but not CCR2 is present on microglia from embryonic development throughout adulthood. *J Immunol* **188**, 29–36 (2012).
29. Hinze, A. *et al.* Microglia differentiation using a culture system for the expansion of mice non-dadherent bone marrow stem cells. *J Inflamm* **9**, 12 (2012).
30. Noto, D. *et al.* Development of a culture system to induce microglia-like cells from haematopoitic cells. *Neuropathol Appl Neurobiol.* Doi10.1111/nan.12086. (2013).
31. Guilemini, G. *et al.* Granulocyte macrophage colony stimulating factor stimulates in vitro proliferation of astrocytes derived from simian mature brains. *Glia* **16**, 71–80 (1996).
32. Gomez-Nicola, D. *et al.* Regulation of microglial proliferation during chronic neurodegeneration. *J Neurosci* **33**, 2481–2493 (2013).
33. Schwarz, J. M. & Bilbo, S. D. Sex, glia, and development: interactions in health and disease. *Horm Behgav* **62**, 243–253 (2012).
34. Paradowska-Gorycka, A. & Jurkowska, M. Structure, expression pattern and biological activity of molecular complex TREM-2/DAP12. *Hum Immunol* **74**, 730–737 (2013).
35. Hamerman, J. A., Tchao, N. K., Lowell, C. A. & Lanier, L. L. Enhanced Toll-like receptor responses in the absence of signaling adaptor DAP12. *Nat Immunol* **6**, 579–586 (2005).

Acknowledgments

The authors would like to thank Ms. Mayumi Tanaka and Ms. Mayumi Inenaga for their technical assistances. We appreciate the technical support from Department of Dermatology (Prof. Masutaka Furue) and the Research Support Center, Graduate School of Medical Sciences, Kyushu University. This work was supported by Grant-in-Aid for Scientific Research on (1) the Japan Society for the Promotion of Science (to TAK, MO and SK), (2) Innovative Areas "Glia Assembly" of The Ministry of Education, Culture, Sports, Science, and Technology, Japan (No. 25117011 to SK), (3) the Health and Labour Sciences Research Grant (No. (H24-Seishin-Jitsuyouka (Seishin)-Ippan-001 to SK), (4) Young Principal Investigators' Research Grant of Innovation Center for Medical Redox Navigation, Kyushu University (to TAK), (5) Takeda Science Foundation – Medical Research (to TAK), and (6) SENSHIN Medical Research Foundation (to TAK). The funders had no role in study design, data collection and analysis, decision to publish, or preparation of the manuscript.

Author contributions

All authors contributed substantially to the scientific process leading up to the writing of the present paper. T.A.K., the principal investigator of the present research, and M.O., the first author, created the conception and design of the project and wrote the protocol. The performance of experiments and the data analysis/interpretation were performed by M.O., T.A.K., D.S., N.S., K.H. and N.S. M.O. wrote the first draft of the manuscript. Clinical recruitments were conducted by R.H., K.S., T.Y., K.H. and N.S. Critical revisions of the manuscript were made by T.A.K., D.M., H.U. and S.K. All authors have approved to submit the final manuscript.

Additional information

Supplementary information accompanies this paper at http://www.nature.com/scientificreports

Competing financial interests: The authors declare no competing financial interests.

How to cite this article: Ohgidani, M. *et al.* Direct induction of ramified microglia-like cells from human monocytes: Dynamic microglial dysfunction in Nasu-Hakola disease. *Sci. Rep.* **4**, 4957; DOI:10.1038/srep04957 (2014).

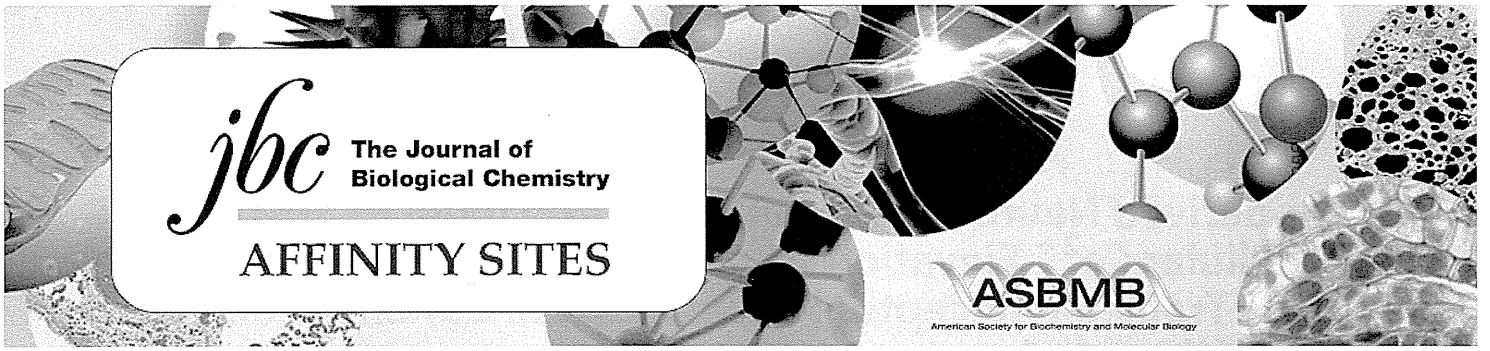

Immunology:

Brain-derived Neurotrophic Factor (BDNF) Induces Sustained Intracellular Ca^{2+} Elevation through the Up-regulation of Surface Transient Receptor Potential 3 (TRPC3) Channels in Rodent Microglia

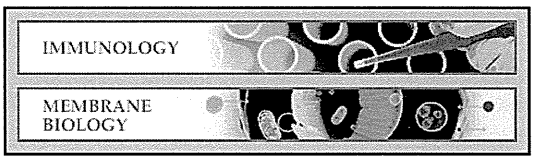

Yoshito Mizoguchi, Takahiro A. Kato, Yoshihiro Seki, Masahiro Ohgidani, Noriaki Sagata, Hideki Horikawa, Yusuke Yamauchi, Mina Sato-Kasai, Kohei Hayakawa, Ryuji Inoue, Shigenobu Kanba and Akira Monji

J. Biol. Chem. 2014, 289:18549-18555.
doi: 10.1074/jbc.M114.555334 originally published online May 8, 2014

THE JOURNAL OF BIOLOGICAL CHEMISTRY VOL. 289, NO. 26, pp. 18549–18555, June 27, 2014

Brain-derived Neurotrophic Factor (BDNF) Induces Sustained Intracellular Ca^{2+} Elevation through the Up-regulation of Surface Transient Receptor Potential 3 (TRPC3) Channels in Rodent Microglia*

Received for publication, February 1, 2014 Published, JBC Papers in Press, May 8, 2014, DOI 10.1074/jbc.M114.555334

Yoshito Mizoguchi[‡1], **Takahiro A. Kato**[§¶], **Yoshihiro Seki**[§], **Masahiro Ohgidani**[§¶], **Noriaki Sagata**[§¶], **Hideki Horikawa**[§], **Yusuke Yamauchi**[§], **Mina Sato-Kasai**[§], **Kohei Hayakawa**[§], **Ryuji Inoue**[‖], **Shigenobu Kanba**[§], **and Akira Monji**[‡]

From the [‡]*Department of Psychiatry, Faculty of Medicine, Saga University, 5-1-1 Nabeshima, Saga 849-8501, Japan, the* [§]*Department of Neuropsychiatry, Graduate School of Medical Sciences, Kyushu University, 3-1-1 Maidashi, Higashi-ku, Fukuoka 812-8582, Japan, the* [¶]*Innovation Center for Medical Redox Navigation, Kyushu University, 3-1-1 Maidashi, Higashi-ku, Fukuoka 812-8582, Japan, and the* [‖]*Department of Physiology, Fukuoka University School of Medicine, 7-45-1 Nanakuma, Jyonan-ku, Fukuoka 812-0180, Japan*

Background: BDNF and Ca^{2+} mobilization is important for microglial function.
Results: We showed BDNF elevates intracellular Ca^{2+} through TRPC3 channels.
Conclusion: TRPC3 is important for BDNF suppression of microglial activation.
Significance: TRPC3 might be important for the treatment of psychiatric disorders.

Microglia are immune cells that release factors, including proinflammatory cytokines, nitric oxide (NO), and neurotrophins, following activation after disturbance in the brain. Elevation of intracellular Ca^{2+} concentration ($[Ca^{2+}]_i$) is important for microglial functions such as the release of cytokines and NO from activated microglia. There is increasing evidence suggesting that pathophysiology of neuropsychiatric disorders is related to the inflammatory responses mediated by microglia. Brain-derived neurotrophic factor (BDNF) is a neurotrophin well known for its roles in the activation of microglia as well as in pathophysiology and/or treatment of neuropsychiatric disorders. In this study, we sought to examine the underlying mechanism of BDNF-induced sustained increase in $[Ca^{2+}]_i$ in rodent microglial cells. We observed that canonical transient receptor potential 3 (TRPC3) channels contribute to the maintenance of BDNF-induced sustained intracellular Ca^{2+} elevation. Immunocytochemical technique and flow cytometry also revealed that BDNF rapidly up-regulated the surface expression of TRPC3 channels in rodent microglial cells. In addition, pretreatment with BDNF suppressed the production of NO induced by tumor necrosis factor α (TNFα), which was prevented by co-adiministration of a selective TRPC3 inhibitor. These suggest that BDNF induces sustained intracellular Ca^{2+} elevation through the up-regulation of surface TRPC3 channels and TRPC3 channels could be important for the BDNF-induced suppression of the NO production in activated microglia. We show that TRPC3 channels could also play important roles in microglial functions, which might be important for the regulation of inflammatory responses and may also be involved in the pathophysiology and/or the treatment of neuropsychiatric disorders.

Microglia are immune cells that release proinflammatory cytokines, nitric oxide (NO), and neurotrophins, when they are activated in response to brain injury or immunological stimuli (1). There is increasing evidence suggesting that pathophysiology of neuropsychiatric disorders is related to inflammatory responses mediated by microglial cells (2, 3).

In the rodent brain, microglial cells secrete brain-derived neurotrophic factor (BDNF), and BDNF promotes the proliferation and survival of microglia themselves (4). In addition, pretreatment with BDNF suppressed the release of NO from murine microglial cells activated by IFN-γ (5). To date, BDNF is also well known for its involvement in the pathophysiology of neuropsychiatric disorders (4, 5).

Elevation of intracellular Ca^{2+} is important in activation of microglial cell functions, including proliferation, release of NO, and migration (1). We have reported previously that BDNF induces a sustained increase in intracellular Ca^{2+} concentration ($[Ca^{2+}]_i$) through the activation of the phospholipase C (PLC)[2] pathway in rodent microglial cells (5). We also tested the effect of 2-aminoethoxydiphenyl borate or SKF-96365, both of which can inhibit canonical transient receptor potential (TRPC) channels (6, 7) and showed that sustained activation of TRPC channels occurred after a brief treatment with BDNF and contributed to the maintenance of BDNF-induced sustained intracellular Ca^{2+} elevation (5).

In this study, we examined whether TRPC3 channels contribute to the maintenance of BDNF-induced sustained intra-

* This work was supported by research grants from the Ministry of Education, Culture, Sports, Science, and Technology of Japan (to Y. M., T. A. K., S. K., and A. M.).

[1] To whom correspondence should be addressed: Dept. of Neuropsychiatry, Faculty of Medicine, Saga University, 5-1-1 Nabeshima, Saga 849-8501, Japan. Tel.: 81-952-34-2304; Fax: 81-952-34-2048; E-mail: ymizo@pk2.so-net.ne.jp.

[2] The abbreviations used are: PLC, phospholipase C; TRPC3, canonical transient receptor potential 3; Pyr3, pyrazole compound 3; HAPI, highly aggressive proliferating immortalized; DAF, 4,5-diaminofluorescein.

cellular Ca^{2+} elevation using the pyrazole compound 3 (Pyr3), a selective inhibitor of TRPC3 channels, which does not affect the activity of other TRPC channel members (8, 9), in rodent microglial cells. Although mRNAs of many TRPC channels, including TRPC3, are shown to be expressed in cultured rat microglia (10), this is the first report showing that TRPC3 channels could also play important roles in microglial functions.

EXPERIMENTAL PROCEDURES

Materials—The drugs used in the present study include Fura2-AM, 4,5-diaminofluorescein diacetate, U73122, and human recombinant TNFα (from Sigma) and polyclonal rabbit anti-TRPC3 channel antibody (ACC-016; Alomone Labs, Jerusalem, Israel). Recombinant IFN-γ and mouse GM-CSF were purchased from R&D Systems. Human recombinant BDNF (Sigma) was diluted with the standard external solution to obtain the final concentration (20 ng/ml; 0.73 nM), which is sufficient to promote the proliferation of microglial cells (4, 5). The final concentration of dimethyl sulfoxide was always <0.1%.

Microglial Cells—Primary microglial cells were prepared from the whole brain of 3-day postnatal Sprague-Dawley rats as described previously (5, 11, 12). Primary mixed cells were prepared from the whole brain of 3-day-postnatal Sprague-Dawley rats using a Cell Strainer (BD Biosciences). Primary rat microglial cells were selected after attachment to Aclar film (Nisshin EM) for 2 h in DMEM supplemented with 10% FBS (10% FBS/DMEM). Aclar films were gently washed with PBS and then transferred to fresh 10% FBS/DMEM, and the fresh microglia expanded for 1–2 days. The purity of isolated microglia was assessed by immunocytochemical staining for the microglial marker, Iba-1, and >99% of cells stained positively (13, 14). The 6-3 microglial cells were established from neonatal C57BL/6J (H-2b) mice as described previously (5, 11–14).

The 6-3 cells were cultured in Eagle's minimal essential medium supplemented with 0.3% $NaHCO_3$, 2 mM glutamine, 0.2% glucose, 10 g/ml insulin, and 10% FCS. Cells were maintained at 37 °C in a 10% CO_2, 90% air atmosphere. GM-CSF was supplemented into the culture medium, at a final concentration of 1 ng/ml, to maintain proliferation of the 6-3 cells. Culture medium was renewed twice per week.

The rat microglial cell line, highly aggressive proliferating immortalized (HAPI) cells (15), was kindly donated by Drs. N. P. Morales and F. Hyodo of Kyushu University. The cells were cultured in DMEM (low glucose; Invitrogen), 5% FBS (Hyclone), 4 mM glutamine (Invitrogen), 100 000 units/liter penicillin G, 100 mg/liter streptomycin (Mediatech), and maintained in 5% CO_2 at 37 °C.

siRNA Transfection—To down-regulate TRPC3 channels, siRNA transfection was performed. The 6-3 microglial cells were cultured in growth medium without antibiotics in a 35-mm glass-based dish until 60–80% confluent. TRPC3-targeting siRNA or scrambled control siRNA (sc-42667 and sc-37007, 80 pmol/dish, respectively; Santa Cruz Biotechnology, Santa Cruz, CA) were transfected into 6-3 microglial cells using siRNA transfection reagent (sc-29528, 6 μl/dish; Santa Cruz Biotechnology) in siRNA transfection medium (sc-36868, 1 ml/dish; Santa Cruz Biotechnology) according to the manufacturer's instructions. Six hours after transfection, normal serum and antibiotics were added at final concentrations of 10 and 1%, respectively. The next day, the medium containing transfection mixtures was replaced with fresh growth medium. At 48 h, the transfected cells were used for intracellular Ca^{2+} imaging.

Intracellular Ca^{2+} Imaging—Intracellular Ca^{2+} imaging using Fura-2-AM was performed as reported previously (5, 16, 17). In brief, the experiments were performed in the external standard solution (150 mM NaCl, 5 mM KCl, 2 mM $CaCl_2$, 1 mM $MgCl_2$, 10 mM glucose, and 10 mM HEPES, pH 7.4, with Tris-OH) at room temperature (27 °C). For Fura-2 excitation, the cells were illuminated with two alternating wavelengths, 340 and 380 nm using a computerized system for a rapid dual wavelength Xenon arc. The emitted light was recorded at 510 nm using a cooled CCD camera (Hamamatsu Photonics). The $[Ca^{2+}]_i$ was calculated from the ratio (R) of fluorescence recorded at 340 and 380 nm excitation wavelengths for each pixel within a microglial cell boundary. All data presented were obtained from at least five dishes and three different cell preparations.

Immunocytochemistry—After microglial cells were fixed, indirect immunofluorescence was performed using the following antibodies: polyclonal rabbit anti-TRPC3 channel antibody (ACC-016; Alomone Labs, Jerusalem, Israel), which recognizes intracellular C terminus of mouse TRPC3 channel and mouse anti-CD45 monoclonal antibody. These specimens were incubated in primary antibodies, and FITC- or Texas red-conjugated secondary antibodies were used for detection. Fluorescent images were captured with a fluorescence microscope (Axio Scope A1, Carl Zeiss, Oberkochen, Germany).

Flow Cytometry—Flow cytometry was performed using a FACS Canto II (BD Biosciences) with FACS Diva software (BD Biosciences). Flow cytometry data were analyzed using FlowJo software (Tree Star, San Carios, CA). The HAPI microglial cells were harvested by non-enzymatic cell dissociation solution (Sigma) and cell lifter (Corning). The cells were fixed with 4% paraformaldehyde and permeabilized with 0.1% Triton X-100. After blocking, the cells were stained with anti-TRPC3 antibody (ACC-016). After washing, the cells were stained with Alexa Fluor 488-conjugated secondary antibody (Invitrogen). The fluorescence intensity of the cells was measured.

Intracellular NO Imaging—The microglial cells were loaded with 10 μM 4,5-diaminofluorescein diacetate (Sigma), a cell membrane-permeable dye that binds intracellular NO (18), for 20 min before the measurement. For DAF-2 excitation, the cells were illuminated with a wavelength, 490 nm, using a computerized system. The signal obtained at 490 nm was previously shown to be, among the excitation wavelengths, quantitatively largest and most representative of change in intracellular NO (19). The emitted light was collected at 510 nm using a cooled CCD camera. The intracellular DAF-2 fluorescence intensity (F) was recorded for each pixel within a cell boundary. The ratio (F/F_0) of fluorescence intensity was estimated from the intensity of fluorescence recorded prior to stimulation (F_0).

All data are expressed as the mean ± S.E., and statistical comparisons were made using an unpaired t test. Significance was established at a level of $p < 0.05$.

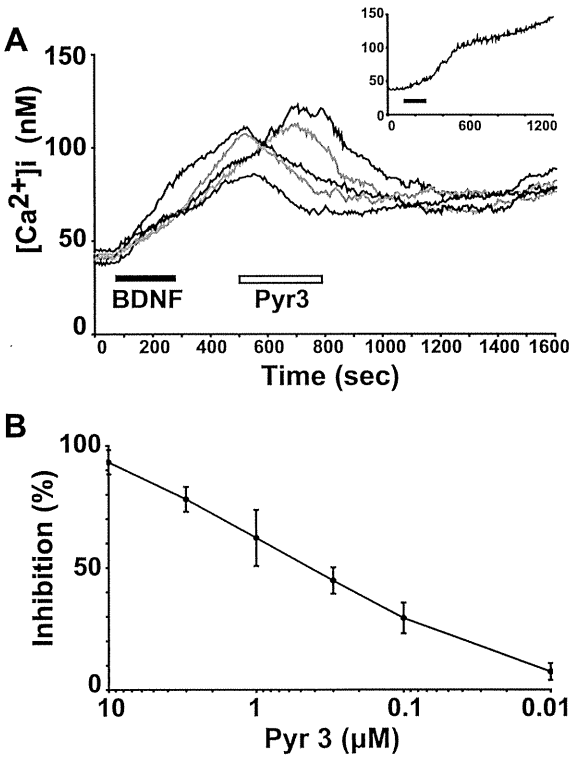

FIGURE 1. **TRPC3 channels contribute to the maintenance of BDNF-induced sustained intracellular Ca^{2+} elevation in rodent microglial cells.** *A*, five representative traces showing the effect of 0.3 μM Pyr3, a selective inhibitor of TRPC3 channels, after the onset of 20 ng/ml BDNF-induced sustained elevation of $[Ca^{2+}]_i$ in primary rat microglial cells. *Inset*, the inset shows a brief (3 min) treatment of BDNF-induced sustained increase in $[Ca^{2+}]_i$ in primary rat microglial cells. The average trace of five $[Ca^{2+}]_i$ traces in response to BDNF is shown. *B*, the dose-response effect of different concentrations of Pyr3 on inhibition of the amplitude of $[Ca^{2+}]_i$ increase obtained 15 min after BDNF treatment in primary rat microglial cells. Values are the mean ± S.E.

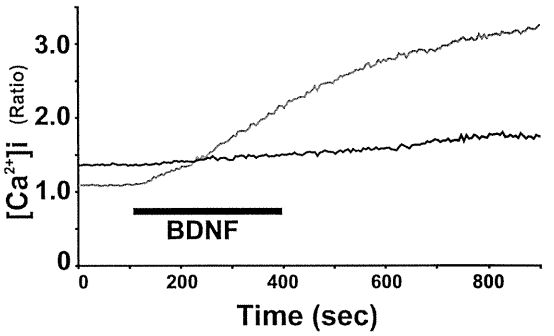

FIGURE 2. **Down-regulation of TRPC3 channels abolished the BDNF-induced elevation of intracellular Ca^{2+} in rodent microglial cells.** The average traces showing the effect of BDNF (20 ng/ml) on intracellular Ca^{2+} mobilization in 6-3 microglial cells transfected with TRPC3-targeting siRNA (*black line*) and scrambled control siRNA (*gray line*). The average trace was determined from 10 representative traces of intracellular Ca^{2+} in each condition.

RESULTS

We have previously reported that BDNF induces sustained increase in intracellular Ca^{2+} in rodent microglial cells (Fig. 1*A*, *inset*) (5). The increase in intracellular Ca^{2+} was sustained for >40 min even after the washout of BDNF until the end of recording. We applied the Pyr3, a selective inhibitor of TRPC3 channels (8, 9), after the onset of BDNF-induced sustained intracellular Ca^{2+} elevation to investigate the involvement of TRPC3 channels in the maintenance of long lasting $[Ca^{2+}]_i$ elevation. After the onset of BDNF-induced intracellular Ca^{2+} elevation, Pyr3 (0.3 μM) was applied and found to suppress the $[Ca^{2+}]_i$ in the 6-3 (n = 35 cells; data not shown) and primary (n = 78 cells; Fig. 1*A*) microglial cells. As shown in Fig. 1*B*, application of Pyr3 suppressed BDNF-induced intracellular Ca^{2+} elevation in a dose-dependent manner with the IC_{50} value of 0.5 μM. We observed that 10 μM Pyr3 suppressed the $[Ca^{2+}]_i$ to near basal levels in the 6-3 (n = 22) and primary (n = 21) microglial cells.

To confirm the involvement of TRPC3 channels in the BDNF-induced increase in $[Ca^{2+}]_i$, we down-regulated TRPC3 protein expression using siRNA. As expected, down-regulation of TRPC3 with siRNA suppressed the elevation of $[Ca^{2+}]_i$ induced by BDNF (Fig. 2). These indicate that sustained activation of TRPC3 channels could occur after a brief application of BDNF and contribute to the maintenance of BDNF-induced sustained intracellular Ca^{2+} elevation in rodent microglial cells.

Next, we performed immunocytochemistry to examine the association between TRPC3 surface expression and BDNF in rodent microglia. RT-PCR analysis has shown previously that TRPC3 mRNA is expressed in cultured microglial cells derived from rats (10). We also confirmed the same results in primary microglial cells and 6-3 murine microglial cells (data not shown). Although only weak TRPC3 immunoreactivity was observed in somata of control HAPI microglial cells, a dramatic increase in TRPC3 expression was observed in BDNF-treated HAPI microglial cells (Fig. 3, *A* and *B*). Double immunostaining for TRPC3 and CD45 (cytoplasmic staining of immune cells) demonstrated that TRPC3 was strongly stained on the cell surface of HAPI microglial cells after the BDNF application, suggesting that BDNF rapidly up-regulated the surface expression of TRPC3 channels in rodent microglial cells (Fig. 3, *C* and *D*).

To quantify the above-mentioned results, we next examine the effect of BDNF on surface expression of TRPC3 channels in HAPI microglial cells using flow cytometry. We observed that BDNF rapidly increased the relative expression of surface TRPC3 channels in HAPI microglial cells (n = 3; Fig. 4). Altogether, these indicate that BDNF induces sustained intracellular Ca^{2+} elevation possibly through the up-regulation of surface TRPC3 channels in rodent microglial cells.

We have previously shown that the activation of PLC is involved in the induction of BDNF-induced intracellular Ca^{2+} elevation in rodent microglial cells (5). In the next examination, we observed that pretreatment of U73122 (5 μM), a membrane-permeable specific PLC inhibitor, significantly reduced the amplitude of BDNF-induced increase in relative expression of surface TRPC3 channels in HAPI microglial cells (n = 3; Fig. 4). Thus, the activation of PLC could also be important for the up-regulation of surface TRPC3 channels induced by BDNF in rodent microglial cells.

We have previously reported that pretreatment with BDNF suppressed the release of NO from murine microglial cells activated by IFN-γ (5). In addition, pretreatment of BDNF suppressed the IFN-γ-induced elevation of $[Ca^{2+}]_i$, along with a

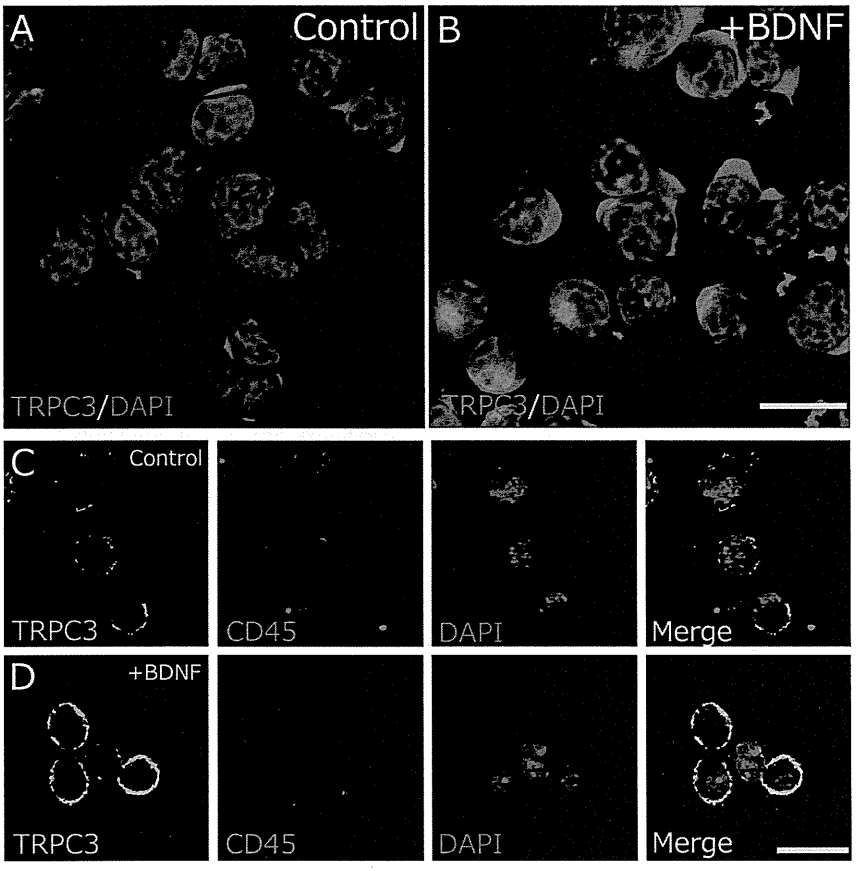

FIGURE 3. **BDNF up-regulates the surface expression of TRPC3 channels in rodent microglial cells.** TRPC3 (*red*) is markedly up-regulated in the BDNF-treated (20 ng/ml, 10 min) HAPI cells (*B*) compared with control cells (*A*). *C* and *D*, two representative confocal images of HAPI microglial cells showing substantial staining of TRPC3 (*green*) and CD45 (*red*). The surface expression of TRPC3 is up-regulated in BDNF-treated HAPI cells (*D*) compared with control cells (*C*). The nuclei are stained with 4′,6-diamidino-2-phenylindole (*blue*). The *scale bars* indicate 20 μm.

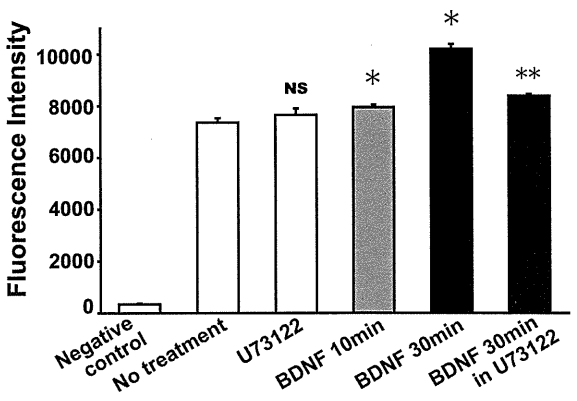

FIGURE 4. **Quantification of the effect of BDNF on the surface expression of TRPC3 channels in rodent microglial cells.** Flow cytomety showing that treatment of BDNF (20 ng/ml) rapidly increased the fluorescence intensity of surface expression of TRPC3 channels in HAPI microglial cells. In contrast, pretreatment of U73122 (5 μM), a membrane-permeable specific PLC inhibitor, significantly reduced the amplitude of BDNF-induced increase in the expression of surface TRPC3 channels in HAPI microglial cells. *, $p < 0.05$ *versus* no treatment; **, $p < 0.01$ *versus* BDNF (30 min). Negative control was obtained from secondary antibody alone. *NS*, nonsignificant.

rise in basal $[Ca^{2+}]_i$ in rodent microglial cells (5). Thus, BDNF-induced elevation of basal levels of $[Ca^{2+}]_i$ could regulate the microglial intracellular signal transduction to suppress the release of NO induced by IFN-γ (4, 5). We next tested whether TRPC3 channels could be important for the BDNF-induced suppression of NO production in rodent microglial cells.

In the present study, 50 units/ml IFN-γ induced sustained intracellular Ca^{2+} elevation in both 6-3 and primary microglial cells as reported previously (data not shown) (5). After the onset of IFN-γ-induced intracellular Ca^{2+} elevation, 3 μM Pyr3 was applied and found to suppress the $[Ca^{2+}]_i$ to near basal levels in the 6-3 ($n = 24$; data not shown) and primary ($n = 47$; Fig. 5*A*) microglial cells. Thus, TRPC3 channels could also contribute to the maintenance of IFN-γ-induced sustained intracellular Ca^{2+} elevation in rodent microglial cells used in this study.

TNFα, one of the proinflammatory cytokines, was shown to induce a gradual increase in intracellular Ca^{2+} in cultured astrocytes at a concentration of 2 μg/ml (20). In the present study, 2 μg/ml TNFα rapidly increased $[Ca^{2+}]_i$ in both 6-3 ($n = 23$; data not shown) and primary microglial cells ($n = 41$; data not shown). Once the intracellular Ca^{2+} level rose, it gradually increased without attenuation even after the washout of TNFα until the end of recording. Interestingly, 3 μM Pyr3 applied after the onset of TNFα-induced intracellular Ca^{2+} elevation did not affect $[Ca^{2+}]_i$ in 6-3 ($n = 21$) and primary ($n = 58$; Fig. 5*B*) microglial cells. These suggest that TRPC3 channels could not be important for the mainte-

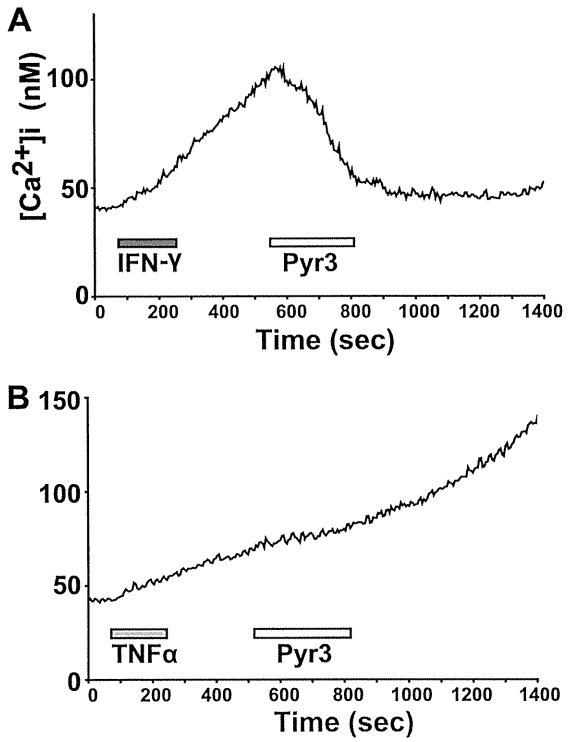

FIGURE 5. **TRPC3 channels are not involved in TNFα-induced sustained intracellular Ca^{2+} elevation in rodent microglial cells.** *A* and *B*, an average trace showing the effect of the 3 μM Pyr3 after the onset of 50 units/ml IFN-γ-induced or 2 μg/ml TNFα-induced sustained elevation of $[Ca^{2+}]_i$ in primary rat microglial cells. Each panel demonstrates the average trace determined from 10 representative traces of $[Ca^{2+}]_i$ in each condition.

nance of TNFα-induced sustained intracellular Ca^{2+} elevation in rodent microglial cells we used.

We next tested the effect of TNFα on intracellular NO mobilization, using DAF-2 imaging to detect endogenously produced NO in rodent microglia. An application of 2 μg/ml TNFα induced a gradual increase in DAF-2 fluorescence in both 6-3 (n = 101; Fig. 6*A*) and primary (n = 45; data not shown) microglial cells tested. The reaction between DAF-2 and NO is shown to be irreversible and the accumulated level of DAF-2 fluorescence reflects the total amount of intracellular NO production (18, 21). We observed that the increase in intracellular DAF-2 fluorescence was sustained for > 40 min even after the washout of TNFα until the end of recording. Additionally, in the presence of 50 μM L-N6-(1-iminoethyl)lysine, a membrane-permeable selective inhibitor of inducible nitric oxide synthase (22), TNFα failed to elevate the DAF-2 fluorescence in both 6-3 (n = 43) and primary (n = 11) microglial cells (data not shown).

We measured the effect of 24-h pretreatment with BDNF (20 ng/ml) on the production of intracellular NO induced by TNFα in rodent microglia. In 6-3 microglial cells that were pretreated with BDNF for 24 h, TNFα (2 μg/ml) also induced a gradual increase in the DAF-2 fluorescence (Fig. 6*B*). However, pretreatment of BDNF significantly reduced the amplitude of TNFα-induced increase in the DAF-2 fluorescence at 15 min after a treatment of TNFα in 6-3 microglial cells (0.171 ± 0.019, n = 101 in control; 0.019 ± 0.007, n = 27 in 5 ng/ml BDNF; 0.018 ± 0.006, n = 68 in 20 ng/ml BDNF; $p < 0.001$; Fig. 6*D*). In contrast, 24 h pretreatment of both BDNF (20 ng/ml) and Pyr3 (0.2 μM) did not reduce the amplitude of TNFα-induced increase in the DAF-2 fluorescence in 6-3 microglial cells

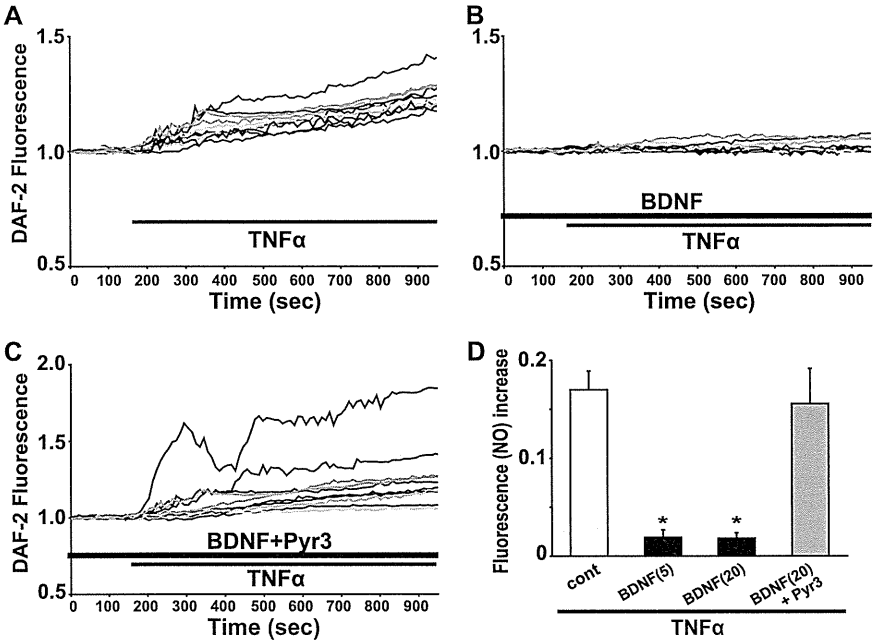

FIGURE 6. **Pretreatment with BDNF suppressed the production of NO induced by TNFα in 6-3 microglial cells.** *A*, 10 representative traces showing the treatment of 2 μg/ml TNFα induced the increase in the DAF-2 fluorescence in murine 6-3 microglial cells. *B*, 10 representative traces showing 24-h pretreatment with 20 ng/ml BDNF suppressed the TNFα-induced increase in the DAF-2 fluorescence in murine 6-3 microglial cells. *C*, 10 representative traces showing 24-h pretreatment with both 20 ng/ml BDNF and 0.2 μM Pyr3 did not suppress the TNFα-induced increase in the DAF-2 fluorescence in murine 6-3 microglial cells. *D*, bar graphs showing that pretreatment with BDNF suppressed the production of NO induced by TNFα treatment and TRPC3 channels could be important for the BDNF-induced suppression of the NO production in murine 6-3 microglial cells. BDNF (5) and BDNF (20) mean 5 ng/ml BDNF and 20 ng/ml BDNF for each.

(0.171 ± 0.019, n = 101 in control; 0.156 ± 0.036, n = 69 in BDNF + Pyr3; p = 0.37; Fig. 6, *C* and *D*). These suggest that pretreatment with BDNF suppressed the production of NO induced by TNFα. In addition, TRPC3 channels could be important for the BDNF-induced suppression of NO production in rodent microglial cells.

DISCUSSION

We found that TRPC3 channels mainly contributed to the maintenance of BDNF-induced sustained intracellular Ca^{2+} elevation in rodent microglial cells. In addition, we suggest that TRPC3 channels could be important for BDNF-induced suppression of NO production in rodent microglial cells activated by TNFα.

BDNF-induced elevation of basal levels of $[Ca^{2+}]_i$ could regulate the microglial intracellular signal transduction to suppress the release of NO induced by IFN-γ (4, 5, 23). We herein showed that pretreatment with BDNF also suppressed the production of NO in murine microglial cells activated by TNFα, which was prevented by co-administration of Pyr3. We also found that pretreatment with both BDNF and Pyr3 did not elevate the basal $[Ca^{2+}]_i$ in rodent microglial cells (data not shown). These suggest that BDNF-induced elevation of basal levels of $[Ca^{2+}]_i$ mediated by TRPC3 channels could be important for the BDNF-induced suppression of NO production in rodent microglial cells.

We observed an application of Pyr3 did not suppress the elevation of $[Ca^{2+}]_i$ induced by TNFα in rodent microglial cells. TRPM2 channels, a member of the melastatin subfamily of TRP channels, are shown to mediate the TNFα-induced intracellular $[Ca^{2+}]_i$ oscillation (24), suggesting that TRPM2 channels might be involved in the TNFα-induced sustained $[Ca^{2+}]_i$ increase in rodent microglial cells.

We have recently reported that pretreatment with antidepressants (13) or antipsychotics (14, 25) significantly inhibits the release of NO from activated microglia. In this study, we observed that pretreatment with BDNF significantly inhibited the production of NO in microglia activated by TNFα. TNFα plays a key role in the induction of sickness behaviors (26) and also in the development of depressive symptoms (27). Thus, this would suggest that BDNF might have an anti-inflammatory effect through the inhibition of microglial activation and could be useful for the treatment of neuropsychiatric disorders. We need to further examine the mechanism underlying the up-regulation of surface TRPC3 channels induced by BDNF in rodent microglial cells.

Acknowledgments—We thank Drs. Shigeki Kiyonaka and Yasuo Mori of Kyoto University for providing us with the pyrazole compound 3 and also thank Dr. Makoto Sawada of Nagoya University for providing us with the microglial cell line, 6-3.

REFERENCES

1. Kettenmann, H., Hanisch, U. K., Noda, M., and Verkhratsky, A. (2011) Physiology of microglia. *Physiol. Rev.* **91,** 461–553
2. Monji, A., Kato, T. A., Mizoguchi, Y., Horikawa, H., Seki, Y., Kasai, M., Yamauchi, Y., Yamada, S., and Kanba, S. (2013) Neuroinflammation in schizophrenia especially focused on the role of microglia. *Prog. Neuropsychopharmacol. Biol. Psychiatry* **42,** 115–121
3. Kato, T. A., Yamauchi, Y., Horikawa, H., Monji, A., Mizoguchi, Y., Seki, Y., Hayakawa, K., Utsumi, H., and Kanba, S. (2013) Neurotransmitters, psychotropic drugs and microglia: clinical implications for psychiatry. *Curr. Med. Chem.* **20,** 331–344
4. Mizoguchi, Y., Monji, A., Kato, T. A., Horikawa, H., Seki, Y., Kasai, M., Kanba, S., and Yamada, S. (2011) Possible role of BDNF-induced microglial intracellular Ca^{2+} elevation in the pathophysiology of neuropsychiatric disorders. *Mini Rev. Med. Chem.* **11,** 575–581
5. Mizoguchi, Y., Monji, A., Kato, T., Seki, Y., Gotoh, L., Horikawa, H., Suzuki, S. O., Iwaki, T., Yonaha, M., Hashioka, S., and Kanba, S. (2009) Brain-derived neurotrophic factor induces sustained elevation of intracellular Ca^{2+} in rodent microglia. *J. Immunol.* **183,** 7778–7786
6. Amaral, M. D., and Pozzo-Miller, L. (2007) TRPC3 channels are necessary for brain-derived neurotrophic factor to activate a nonselective cationic current and to induce dendritic spine formation. *J. Neurosci.* **27,** 5179–5189
7. Bootman, M. D., Collins, T. J., Mackenzie, L., Roderick, H. L., Berridge, M. J., and Peppiatt, C. M. (2002) 2-aminoethoxydiphenyl borate (2-APB) is a reliable blocker of store-operated Ca^{2+} entry but an inconsistent inhibitor of $InsP_3$-induced Ca^{2+} release. *FASEB J.* **16,** 1145–1150
8. Kiyonaka, S., Kato, K., Nishida, M., Mio, K., Numaga, T., Sawaguchi, Y., Yoshida, T., Wakamori, M., Mori, E., Numata, T., Ishii, M., Takemoto, H., Ojida, A., Watanabe, K., Uemura, A., Kurose, H., Morii, T., Kobayashi, T., Sato, Y., Sato, C., Hamachi, I., and Mori, Y. (2009) Selective and direct inhibition of TRPC3 channels underlies biological activities of a pyrazole compound. *Proc. Natl. Acad. Sci. U.S.A.* **106,** 5400–5405
9. Kim, M. S., Lee, K. P., Yang, D., Shin, D. M., Abramowitz, J., Kiyonaka, S., Birnbaumer, L., Mori, Y., and Muallem, S. (2011) Genetic and pharmacologic inhibition of the Ca^{2+} influx channel TRPC3 protects secretory epithelia from Ca^{2+}-dependent toxicity. *Gastroenterology* **140,** 2107–2115
10. Ohana, L., Newell, E. W., Stanley, E. F., and Schlichter, L. C. (2009) The Ca^{2+} release-activated Ca^{2+} current (I(CRAC)) mediates store-operated Ca^{2+} entry in rat microglia. *Channels* **3,** 129–139
11. Kato, T., Mizoguchi, Y., Monji, A., Horikawa, H., Suzuki, S. O., Seki, Y., Iwaki, T., Hashioka, S., and Kanba, S. (2008) Inhibitory effects of aripiprazole on interferon-γ-induced microglial activation via intracellular Ca^{2+} regulation *in vitro*. *J. Neurochem.* **106,** 815–825
12. Seki, Y., Suzuki, S. O., Masui, K., Harada, S., Nakamura, S., Kanba, S., and Iwaki, T. (2011) A simple and high-yield method for preparation of rat microglial cultures utilizing Aclar plastic film. *Neuropathology* **31,** 215–222
13. Horikawa, H., Kato, T. A., Mizoguchi, Y., Monji, A., Seki, Y., Ohkuri, T., Gotoh, L., Yonaha, M., Ueda, T., Hashioka, S., and Kanba, S. (2010) Inhibitory effects of SSRIs on IFN-γ induced microglial activation through the regulation of intracellular calcium. *Prog. Neuropsychopharmacol. Biol. Psychiatry* **34,** 1306–1316
14. Kato, T. A., Monji, A., Yasukawa, K., Mizoguchi, Y., Horikawa, H., Seki, Y., Hashioka, S., Han, Y. H., Kasai, M., Sonoda, N., Hirata, E., Maeda, Y., Inoguchi, T., Utsumi, H., and Kanba, S. (2011) Aripiprazole inhibits superoxide generation from phorbol-myristate-acetate (PMA)-stimulated microglia *in vitro*: implication for antioxidative psychotropic actions via microglia. *Schizophr. Res.* **129,** 172–182
15. Cheepsunthorn, P., Radov, L., Menzies, S., Reid, J., and Connor, J. R. (2001) Characterization of a novel brain-derived microglial cell line isolated from neonatal rat brain. *Glia* **35,** 53–62
16. Mizoguchi, Y., Ishibashi, H., and Nabekura, J. (2003) The action of BDNF on $GABA_A$ currents changes from potentiating to suppressing during maturation of rat hippocampal CA1 pyramidal neurons. *J. Physiol.* **548,** 703–709
17. Mizoguchi, Y., Kanematsu, T., Hirata, M., and Nabekura, J. (2003) A rapid increase in the total number of cell surface functional GABAA receptors induced by brain-derived neurotrophic factor in rat visual cortex. *J. Biol. Chem.* **278,** 44097–44102
18. Kojima, H., Nakatsubo, N., Kikuchi, K., Kawahara, S., Kirino, Y., Nagoshi, H., Hirata, Y., and Nagano, T. (1998) Detection and imaging of nitric oxide with novel fluorescent indicators: diaminofluoresceins. *Anal. Chem.* **70,** 2446–2453

19. Patel, V. H., Brack, K. E., Coote, J. H., and Ng, G. A. (2008) A novel method of measuring nitric-oxide-dependent fluorescence using 4,5-diaminofluorescein (DAF-2) in the isolated Langendorff-perfused rabbit heart. *Pflugers Archiv.* **456,** 635–645
20. Köller, H., Thiem, K., and Siebler, M. (1996) Tumour necrosis factor-α increases intracellular Ca^{2+} and induces a depolarization in cultured astroglial cells. *Brain* **119,** 2021–2027
21. Kalinchuk, A. V., McCarley, R. W., Porkka-Heiskanen, T., and Basheer, R. (2010) Sleep deprivation triggers inducible nitric oxide-dependent nitric oxide production in wake-active basal forebrain neurons. *J. Neurosci.* **30,** 13254–13264
22. Moore, W. M., Webber, R. K., Jerome, G. M., Tjoeng, F. S., Misko, T. P., and Currie, M. G. (1994) L-N6-(1-iminoethyl)lysine: a selective inhibitor of inducible nitric oxide synthase. *J. Med. Chem.* **37,** 3886–3888
23. Hoffmann, A., Kann, O., Ohlemeyer, C., Hanisch, U. K., and Kettenmann, H. (2003) Elevation of basal intracellular calcium as a central element in the activation of brain macrophages (microglia): suppression of receptor-evoked calcium signaling and control of release function. *J. Neurosci.* **23,** 4410–4419
24. Nazıroğlu, M. (2011) TRPM2 cation channels, oxidative stress and neurological diseases: where are we now? *Neurochem. Res.* **36,** 355–366
25. Kato, T. A., Monji, A., Mizoguchi, Y., Hashioka, S., Horikawa, H., Seki, Y., Kasai, M., Utsumi, H., and Kanba, S. (2011) Anti-inflammatory properties of antipsychotics via microglia modulations: are antipsychotics a "fire extinguisher" in the brain of schizophrenia? *Mini. Rev. Med. Chem.* **11,** 565–574
26. Simen, B. B., Duman, C. H., Simen, A. A., and Duman, R. S. (2006) TNFα signaling in depression and anxiety: behavioral consequences of individual receptor targeting. *Biol. Psychiatry.* **59,** 775–785
27. Dantzer, R., O'Connor, J. C., Freund, G. G., Johnson, R. W., and Kelley, K. W. (2008) From inflammation to sickness and depression: when the immune system subjugates the brain. *Nat. Rev. Neurosci.* **9,** 46–56

LETTER TO THE EDITOR

Minocycline, a Microglial Inhibitor, Diminishes Terminal Patients' Delirium?

Delirium, causing diverse mental and behavioral symptoms due to disturbance of consciousness, is very common, especially in geriatric patients.[1] In palliative medicine, delirium distresses patients, their family, and caregivers,[2] worsening the quality of the end stages of life. We herein report two cases of successful treatment of multifactorial delirium in patients with terminal cancer by a tetracycline antibiotic, minocycline.

A 70-year-old man with hepatocellular carcinoma with multiple metastases was admitted to a palliative care inpatient unit (Day 0). On the first night of his hospital stay, he had insomnia, disorientation, disconnected speech, and visual hallucinations. Although his consciousness had been clear in the daytime on Day 1, he had recurrent disorientation and visual hallucinations from the evening. On the morning on Day 2, he was diagnosed with delirium by a psychiatrist according to the Diagnostic and Statistical Manual of Mental Disorders, Fourth Edition, Text Revision (DSM-IV-TR). The Memorial Delirium Assessment Scale (MDAS) score was 11/30. He had developed delirium along with hyponatremia, C- reactive protein (CRP) elevation, and a urinary tract infection. Minocycline (150 mg/day) was orally initiated for the urinary tract infection. Subsequently the MDAS score dramatically decreased to 3/30 on Day 3. Thereafter, his consciousness became clear in the daytime. On Day 5, he was judged to have recovered, with a MDAS score of 4/30.

Another case; an 83-year-old man with lung squamous cell carcinoma with bone and skin metastases was admitted to a palliative care unit for the treatment of chronic aspiration pneumonia (Day 0). Laboratory test results showed hypoalbuminemia, hyponatremia, hypercalcemia, and a high CRP level. Oxycodone was increased from 80 mg/day to 120 mg/day on Day 1. That night he mistakenly took a TV remote to be a microphone, and had insomnia and disconnected speech. On Day 2, he had acute-onset disorientation and disturbance of attention with a MDAS score of 9/30. In accordance with the DSM-IV-TR, a psychiatrist diagnosed him with delirium attributed to multiple factors including aspiration pneumonia. Minocycline (150 mg/day) was orally administered. After starting minocycline, disconnected speech immediately disappeared. He gradually awoke from the afternoon on Day 3 with a MDAS score of 7/30 and was judged to have recovered from the delirious state with a MDAS score of 5/30 on Days 4 and 5.

Treatment for delirium remains to be established, though delirious symptoms, such as delusions and hallucinations, are generally treated with antipsychotics.[3] These two cases showed immediate recovery from delirium by minocycline treatment without any adverse events, usually caused by antipsychotics. Recently, microglial pathology has been suggested in neuropsychiatric disorders.[4] Minocycline is a bacteriostatic agent with antioxidative and antiapoptotic properties, and its potent anti-inflammatory effects through the suppression of microglial activation in the brain have been highlighted in animal models of neuropsychiatric disorders such as schizophrenia and methamphetamine-related disorders.[5] In fact, minocycline has been reported to be effective for various neuropsychiatric disorders including psychosis.[5] A postmortem study has shown a positive association between microglial activity and delirium,[6] and a novel neuroinflammatory hypothesis of delirium via microglial modulation has been proposed.[7] This hypothesis is underpinned by a recent animal study showing that acute cognitive deficits triggered by systemic inflammation are related to progressive microglial cyclooxygenase-1 expression and prostaglandin synthesis.[8] It has not yet been clarified whether minocycline modulate these pathways, but we suggest that minocycline may be effective for delirium by inhibiting microglial activation via some particular pathways. Further molecular investigations and clinical trials should be initiated to confirm the effect of minocycline on delirium.

Kohei Hayakawa, M.D.
Department of Neuropsychiatry, Graduate School of Medical Sciences, Kyushu University, Fukuoka, Japan
Palliative Care Unit, Kyushu Kosei Nenkin Hospital, Kitakyushu, Japan

Takahiro A. Kato, M.D., Ph.D.
Department of Neuropsychiatry, Graduate School of Medical Sciences, Kyushu University, Fukuoka, Japan

Innovation Center for Medical Redox Navigation, Kyushu University, Japan
e-mail: takahiro@npsych.med.kyushu-u.ac.jp

Masaomi Kohjiro, M.D.
Palliative Care Unit, Kyushu Kosei Nenkin Hospital, Kitakyushu, Japan

Akira Monji, M.D., Ph.D.
Department of Neuropsychiatry, Saga Medical School Faculty of Medicine, Saga University, Saga, Japan

Shigenobu Kanba, M.D., Ph.D.
Department of Neuropsychiatry, Graduate School of Medical Sciences, Kyushu University, Fukuoka, Japan

References

1. Cheong JA: Diagnosis, risk factors, predisposing factors, and predictive models of delirium. Am J Geriatr Psychiatry 2013; 21: 931–934
2. Breitbart W, Alici Y: Agitation and delirium at the end of life: "We couldn't manage him". JAMA 2008; 300(24): 2898–2910
3. Inouye SK: Delirium in older persons. N Engl J Med 2006; 354(11):1157–1165
4. Kato TA, Yamauchi Y, Horikawa H, et al: Neurotransmitters, psychotropic drugs and microglia: clinical implications for psychiatry. Curr Med Chem 2013; 20(3): 331–344
5. Hashimoto K, Ishima T, Fujita Y, et al: Antibiotic drug minocycline: a potential therapeutic drug for methamphetamine-related disorders. Nihon Arukoru Yakubutsu Igakkai Zasshi [Japanese Journal of Alcohol Studies & Drug Dependence] 2013; 48:118–125
6. Munster BC, Aronica E, Zwinderman AH, et al: Neuroinflammation in delirium: a postmortem case-control study. Rejuvenation Res 2011; 14(6):615–622
7. van Gool WA, van de Beek D, Eikelenboom P: Systemic infection and delirium: when cytokines and acetylcholine collide. Lancet 2010; 375(9716): 773–775
8. Griffin EW, Skelly DT, Murray CL, et al: Cyclooxygenase-1-dependent prostaglandins mediate susceptibility to systemic inflammation-induced acute cognitive dysfunction. J Neurosci 2013; 33: 15248–15258

OPEN ACCESS Freely available online

PLOS ONE

Resequencing and Association Analysis of *PTPRA*, a Possible Susceptibility Gene for Schizophrenia and Autism Spectrum Disorders

Jingrui Xing[1], Chenyao Wang[1], Hiroki Kimura[1], Yuto Takasaki[1], Shohko Kunimoto[1], Akira Yoshimi[1], Yukako Nakamura[1], Takayoshi Koide[1], Masahiro Banno[1], Itaru Kushima[1], Yota Uno[1], Takashi Okada[1], Branko Aleksic[1]*, Masashi Ikeda[2], Nakao Iwata[2], Norio Ozaki[1]

1 Department of Psychiatry, Nagoya University Graduate School of Medicine, Nagoya, Japan, **2** Department of Psychiatry, School of Medicine, Fujita Health University, Toyoake, Aichi, Japan

Abstract

Background: The *PTPRA* gene, which encodes the protein RPTP-α, is critical to neurodevelopment. Previous linkage studies, genome-wide association studies, controlled expression analyses and animal models support an association with both schizophrenia and autism spectrum disorders, both of which share a substantial portion of genetic risks.

Methods: We sequenced the protein-encoding areas of the *PTPRA* gene for single nucleotide polymorphisms or small insertions/deletions (InDel) in 382 schizophrenia patients. To validate their association with the disorders, rare (minor allele frequency <1%), missense mutations as well as one InDel in the 3′UTR region were then genotyped in another independent sample set comprising 944 schizophrenia patients, 336 autism spectrum disorders patients, and 912 healthy controls.

Results: Eight rare mutations, including 3 novel variants, were identified during the mutation-screening phase. In the following association analysis, L59P, one of the two missense mutations, was only observed among patients of schizophrenia. Additionally, a novel duplication in the 3′UTR region, 174620_174623dupTGAT, was predicted to be located within a Musashi Binding Element.

Major Conclusions: No evidence was seen for the association of rare, missense mutations in the *PTPRA* gene with schizophrenia or autism spectrum disorders; however, we did find some rare variants with possibly damaging effects that may increase the susceptibility of carriers to the disorders.

Citation: Xing J, Wang C, Kimura H, Takasaki Y, Kunimoto S, et al. (2014) Resequencing and Association Analysis of *PTPRA*, a Possible Susceptibility Gene for Schizophrenia and Autism Spectrum Disorders. PLoS ONE 9(11): e112531. doi:10.1371/journal.pone.0112531

Editor: Namik Kaya, King Faisal Specialist Hospital and Research center, Saudi Arabia

Received April 11, 2014; **Accepted** September 30, 2014; **Published** November 13, 2014

Data Availability: The authors confirm that all data underlying the findings are fully available without restriction. All relevant data are within the paper and its Supporting Information files.

Funding: Funding for this study was provided by research grants from the Ministry of Education, Culture, Sports, Science and Technology of Japan; the Ministry of Health, Labor and Welfare of Japan; Grant-in-Aid for "Integrated research on neuropsychiatric disorders" carried out under the Strategic Research Program for Brain Sciences by the Ministry of Education, Culture, Sports, Science and Technology of Japan; Grant-in-Aid for Scientific Research on Innovative Areas, "Glial assembly: a new regulatory machinery of brain function and disorders"; and Grant-in-Aid for Scientific Research on Innovative Areas (Comprehensive Brain Science Network) from the Ministry of Education, Science, Sports and Culture of Japan. The funders had no role in study design, data collection and analysis, decision to publish, or preparation of the manuscript.

Competing Interests: Dr. Aleksic is a PLOS ONE Editorial Board member, and that does not alter the authors' adherence to PLOS ONE Editorial policies and criteria.

* Email: branko@med.nagoya-u.ac.jp

Introduction

Schizophrenia (SCZ) is a genetically heterogeneous disorder with heritability estimated at up to 80% [1]. In recent years, although research projects such as large-scale genome-wide association studies (GWAS) have focused on common variants, they have failed to explain the majority of the heritability of SCZ [2,3]. Subsequently, great interest has been drawn to rare (minor allele frequency, MAF <1%) missense mutations as potentially important contributing factors to the 'missing heritability' [4,5]. The concept of Autism Spectrum Disorders (ASD) has been defined in the newly released Diagnostic and Statistical Manual of Mental Disorders version 5 (DSM-5) to include previous diagnoses of autistic disorder, Asperger's syndrome and PDD-NOS (pervasive developmental disorders not otherwise specified) [6]. Both SCZ and ASD are recognized as neurodevelopmental disorders, and are reported to have a major overlap of genetic risk, especially from *de novo*, deleterious mutations, [7–10]although further research concerning implicated loci and/or genetic risk factors (i.e., copy number variants [CNV], insertion/deletions, and single nucleotide variants) is required.

The human protein tyrosine phosphatase receptor type A (*PTPRA*) gene encodes the enzyme receptor-type tyrosine-protein phosphatase alpha (RPTP-α), a member of the protein tyrosine phosphatase (PTP) family that is involved in numerous neurodevelopmental processes related to the pathogenesis of SCZ and ASD such as myelination, radial neuronal migration, cortical cytoarchitecture formation and oligodendrocyte differentiation [11–14]. Moreover, RPTP-α is also functionally involved in the *neuregulin 1* (*NRG1*) signaling pathway, which regulates neurodevelopment as well as glutamatergic and gamma-aminobutyric acid–ergic neurotransmission [15–17]. The *NRG1* gene, together with two other genes in the same pathway—*ERBB4*, which encodes a downstream tyrosine kinase receptor[16–18], and *PTPRZ1*, which encodes an *ERBB4*-associated protein tyrosine phosphatase[19]—have been reported by some studies to be associated with SCZ [20–22].

Multiple lines of biological evidence implicate the *PTPRA* gene in the etiology of SCZ or ASD. Previous linkage studies conducted in 270 Irish high-density families ($p = .0382$) and an inbred, Arab Israeli pedigree of 24 members (LOD score = 2.56 at 9.53 cM) have pointed to the area that harbors the gene [23,24]. A GWAS comprising 575 cases and 564 controls of the Japanese ethnicity showed an association between polymorphisms within the *PTPRA* gene and SCZ (best uncorrected $p = .002$), albeit not at the level of genome-wide significance [25]. This result was followed by a replication study of 850 cases and 829 controls, which further confirmed the association ($p = .04$, $p = .0008$ for pooled analysis of first and second stages) [26]. Patients carrying copy number variations (CNVs) within the gene have been reported to suffer from autism, or have delayed language and speech development or stereotypical behaviors [27]. Reduced *PTPRA* expression levels have been observed in postmortem brains from patients with SCZ when compared to brains from healthy controls (13% decrease; $p = .018$). In the same study, a significant difference in the expression of mRNA levels of one alternative splicing variant within the gene ($p = .024$) was discovered in an expression analysis using lymphoblastoid cell lines (LCL) derived from 28 patients with SCZ and 20 healthy controls [26]. *Ptpra* knockout mice have been shown to exhibit neurodevelopmental deficiencies and schizophrenic-like behavioral patterns that are thought to model certain aspects of the disorder in humans. In addition, loss of *Ptpra* function in mice also leads to reduced expression of multiple myelination genes, [26] a phenomenon commonly associated with SCZ [28–32] and ASD [33–35] in human patients.

Given the aforementioned studies suggesting the association between *PTPRA* and SCZ/ASD, we decided to sequence the exonic areas of the gene in search for rare, protein-altering mutations that may further strengthen the evidence implicating *PTPRA* as a risk gene for these neurodevelopmental disorders.

Materials and Methods

Participants

Two independent sample sets were used in this study (Table 1). The first set, comprising 382 SCZ patients (mean age = 53.6±14.2; male = 56.5%;), was sequenced for missense rare variants, including single nucleotide polymorphisms (SNPs), small InDels and splicing site variations. The second, larger set, comprising 944 SCZ patients (mean age = 50.4±15.6, male = 58.7%), 336 ASD patients (mean age = 19.3±10.0, male = 77.1%), and 912 controls (mean age = 39.1±15.9, male = 44.5%), was used for association analysis of variants detected in the first phase.

All participants in this study were recruited in the Nagoya University Hospital and its associated institutes. Patients were included in the study if they (1) met DSM-5 criteria for SCZ or ASD and (2) were physically healthy. Controls were selected from the general population and had no personal or family history of psychiatric disorders (first-degree relatives only based on the subject's interview). The selection was based on the following: (1) questionnaire responses from the subjects themselves during the sample inclusion step; or (2) an unstructured diagnostic interview conducted by an experienced psychiatrist during the blood collection step. All subjects were unrelated, living in the central area of the Honshu island of Japan, and self-identified as members of the Japanese population. The Ethics Committees of the Nagoya University Graduate School of Medicine approved this study. Written informed consent was obtained from all participants. In addition, the patients' capacity to consent was confirmed by a family member when needed. Individuals with a legal measure of reduced capacity were excluded.

Resequencing and Data Analysis

The human *PTPRA* gene is located at Chromosome 20: 2,844,830–3,019,320 and has a total of 28 exons (Ensembl release 73; Genome assembly: GRCh37; Transcript: ENST00000380393) (Fig. 1). We included only coding regions and 3′UTR (exons 8–28) (Fig. 2). Genomic DNA was extracted from whole blood or saliva using QIAGEN QIAamp DNA blood kit or tissue kit (QIAGEN Ltd. Hilden, Germany). Primers for 10 amplicons ranging from lengths of 700 to 3000 bps covering all the target exons were designed with the Primer-BLAST tool by NCBI (http://www.ncbi.nlm.nih.gov/tools/primer-blast/) and tested for validity with UCSC In-Silico PCR (http://genome.ucsc.edu/cgi-bin/hgPcr). The Takara LA taq Kit (Takara Bio Inc. Shiga, Japan) was used for PCR amplification, and products were cleaned up with Illustra Exonuclease I and Alkaline Phosphatase (GE Healthcare & Life Science, Little Chalfont, United Kingdom). After that, Sanger sequencing was performed using the BigDye Terminator v3.1 Cycle Sequencing Kit (Applied Biosystems, Foster City, California, United States). Upon the initial discovery, for all variants, we used Sanger sequencing to confirm the detection.

Table 1. Profiles of participants in the resequencing and association sample sets.

	Sequencing	Association Study				Total
	Schizophrenia	Schizophrenia	ASD	Control	Total	
Total	382	944	336	912	2192	2574
Male	216 (56.5%)	554 (58.7%)	259 (77.1%)	406 (44.5%)	1037 (47.3%)	1253 (48.7%)
Female	166 (43.5%)	369 (39.1%)	77 (22.9%)	503 (55.2%)	1131 (51.6%)	1297 (50.4%)
Mean Age (years)	53.6±14.2	50.4±15.6	19.3±10.0	39.1±15.9	44.9±18.7	42.3±18.7

Note: Some samples in the association study group were not identified by sex.

doi:10.1371/journal.pone.0112531.t001

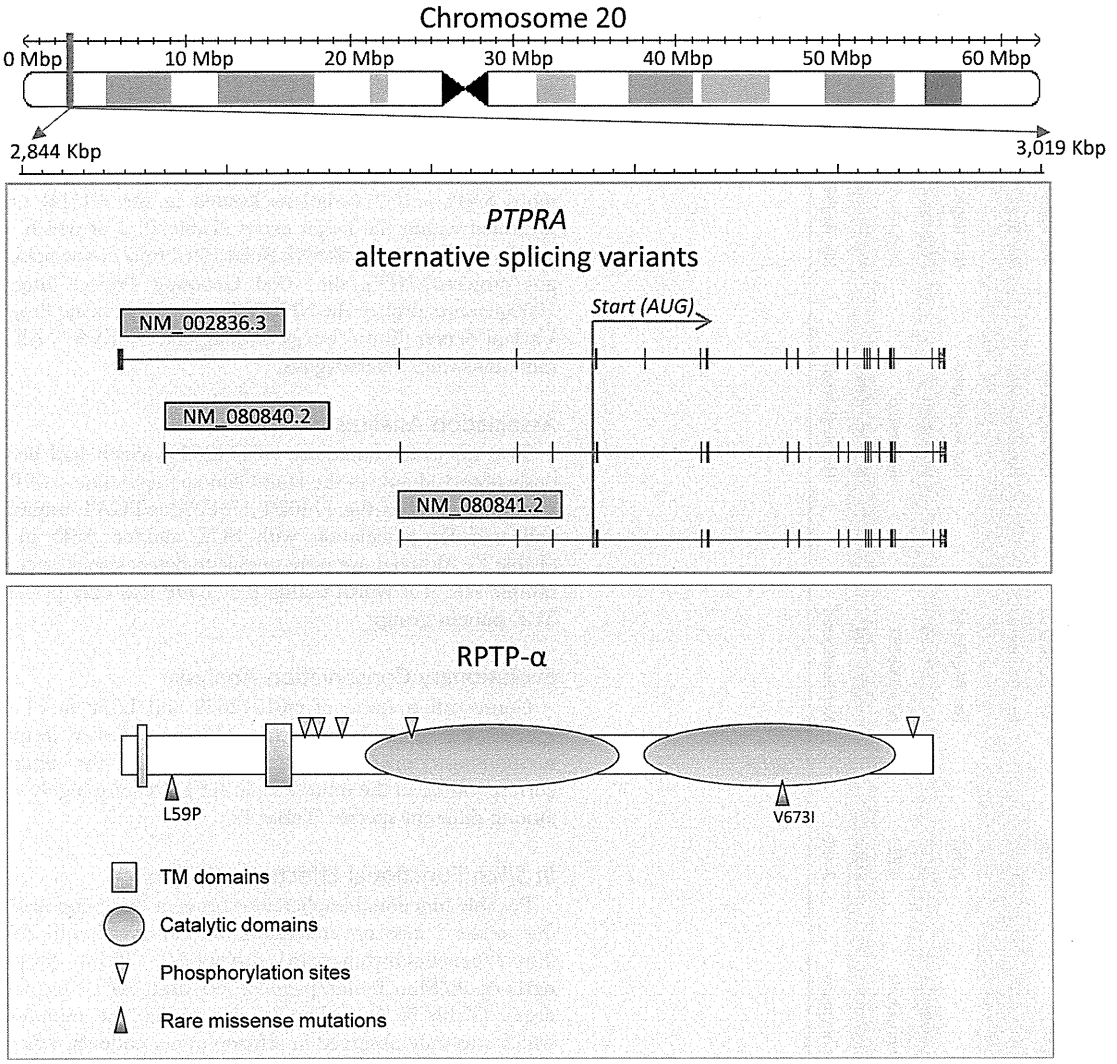

Figure 1. Structure of the *PTPRA* gene, RPTP-α, and position of discovered rare missense mutations.
doi:10.1371/journal.pone.0112531.g001

Sequenced samples were read on an Applied Biosystems 3130xL Genetic Analyzer. Mutation detection was performed with Mutation Surveyor (Softgenetics, State College, PA, USA). The mutation calls were then revalidated for confidence.

Association Analysis

Missense and 3′UTR mutations with MAF<1% were picked up for the association stage. Due to the altering effects that splice site variants have on the structure of mRNAs, and consequently the production of the protein, [36,37] they were also included in the association analysis if they met the MAF criteria.

Custom TaqMan SNP genotyping assays were designed and ordered from Applied Biosystems. Allelic discrimination analysis was performed on an ABI PRISM 7900HT Sequence Detection System (Applied Biosystems, Foster City, California, United States). Differences in allele and genotype frequencies of the mutations were compared between SCZ patients/controls and ASD patients/

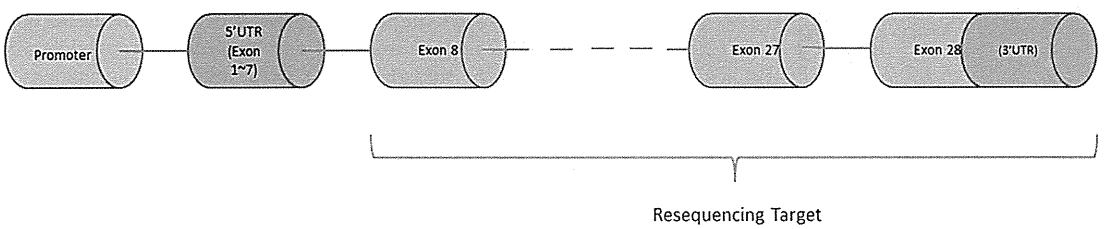

Figure 2. Targeted sequencing areas of the *PTPRA* Gene.
doi:10.1371/journal.pone.0112531.g002

Table 2. Rare exonic mutations identified during the resequencing stage.

Genomic Position [a]	Exon	Base Pair Change [b]	AA Change [c]	Frequency	dbSNP Reference	1000 Genomes	ESP Variant Server
20:3016327	Exon 25	171999G>GA	673V>VI	1/382	rs61742029	Registered	Registered
20:2945609	Exon 9	107281T>TC	59L>LP	2/382	Not Registered	Not Registered	Not Registered
20:3018948	3'UTR	174620_174623 het_dupTGAT	—	1/382	Not Registered	Not Registered	Not Registered
20:3019013	3'UTR	174685A>AT	—	2/382	Not Registered	Not Registered	Not Registered
20:2945649	Exon 9	124753A>AG	Synonymous	4/382	rs138210276	Registered	Registered
20:3005207	Exon 21	160879G>GA	Synonymous	1/382	rs150908061	Registered	Registered
20:3017902	Exon 27	173574G>GT	Synonymous	2/382	rs375917163	Not Registered	Not Registered
20:3017903	Exon 27	173575C>CA	Synonymous	2/382	Not Registered	Not Registered	Not Registered

Notes:
[a]: Based on NCBI build 37.1.
[b]: Based on NCBI Reference Sequence NC_000020.10.
[c]: Based on NCBI Reference Sequence NP_001099043. AA: amino acid.
All mutations are heterozygous.
doi:10.1371/journal.pone.0112531.t002

controls using Fisher's exact test (one-tail), with a threshold of significance set at $p<0.05$.

Results

Mutation Screening Step

Eight rare mutations consisting of 2 missense SNPs, 4 synonymous SNPs and 2 variations located in the 3'UTR area were identified within the target exons (Table 2), 4 of which were not previously reported in dbSNP Build 139 (http://www.ncbi.nlm.nih.gov/projects/SNP/), the 1000 Genomes Project (http://www.1000genomes.org), or the NHLBI Exome Sequencing Project (ESP) Variant Server (http://evs.gs.washington.edu/EVS/). All detected mutations were heterozygous.

Association Analysis

Two missense mutations, rs61742029, which had been previously observed only in the Han Chinese population, L59P, a novel variant, as well as the 174620_174623dupTGAT mutation were validated for association with SCZ and/or ASD in stage 2 (Table 3). Although we were unable to detect significance with our sample sets, it is worth noting that L59P was only present in the SCZ patient group.

Evolutionary Conservation Analysis

Conservation status of rs61742029 and L59P in 11 common species was investigated using Mutation Taster (http://www.mutationtaster.org/). Results showed that the amino acids corresponding to the mutations in RPTP-α were highly conserved among different species (Table 4).

In Silico Functional Effects Prediction

Possible functional implications brought by amino acid changes due to the 2 missense mutations were analyzed with PolyPhen-2 (http://genetics.bwh.harvard.edu/pph2/), PMut (http://www.ngrl.org.uk/Manchester/page/pmut) and SIFT (http://sift.jcvi.org/). (Table 5) According to the results, the mutation L59P, which was only observed in schizophrenia patients, was predicted to be mostly benign, while rs61742029 showed a high probability of pathogenicity in PolyPhen-2.

3'UTR Motif Prediction

174620_174623dupTGAT, a small duplication discovered in the 3'UTR area, was predicted by RegRNA 2.0 (http://regrna2.mbc.nctu.edu.tw) to be located within a human Musashi Binding Element (MBE), an evolutionarily conserved region shown to affect neural cell differentiation through its mRNA translation regulator properties [38].

Clinical Information of the Carriers of Mutation L59P and 174620_174623dupTGAT

The patient carrying the *PTPRA* L59P mutation was a male diagnosed with SCZ at the age of 19. The patient was born in 1947 had a normal course of development during childhood. In early 1966, he started to suffer from auditory hallucinations, and soon withdrew into an indoor lifestyle. His family reported him being irritated when visited, as well as behaving improperly in public. He was promptly diagnosed and admitted to a psychiatry ward in the same year, and spent the rest of his life living in a hospital. A remarkable improvement was observed in his positive symptoms after admission and administration of antipsychotic drugs; however, he remained secluded, hardly communicating with people around him. At the time of his enrollment in the study, he was 162 cm tall

Table 3. Association analysis results of two rare missense mutations and one 3′UTR variant.

Mutation	Genotype Counts (Resequencing) [a]	Genotype Counts (Association)			P Value [b]	
		SZ	ASD	Ctrl	SZ	ASD
171999G>GA, 673V>VI	**0/3/379**	**0/2/942**	**0/2/334**	**0/4/908**	**0.3276**	**0.2829**
101281T>TC, 59L>L/P	0/2/380	0/0/944	0/0/336	0/0/912	1.0000	1.0000
174620_174623het_dupTGAT	0/1/381	0/0/944	0/0/336	0/1/911	0.4914	1.0000

Notes:
[a]: Homozygote of minor allele/heterozygote/homozygote of major allele.
[b]: Calculated using Fisher's exact test, one-tailed.
Ctrl: healthy controls.
doi:10.1371/journal.pone.0112531.t003

and weighed 48 kg. No comorbid physical or mental illnesses were present. He had 3 children, among whom, one daughter had a history of mental disorder. The patient succumbed to pneumonia in the second half of 2013. In a computerized axial tomography (CAT) scan of the head taken a few weeks prior to patient's death, diffuse neocortical atrophy was observed.

The other patient carrying the L59P mutation was a female diagnosed with SCZ at the age of 34. No childhood development abnormalities were reported, but she was noted to have a history of irritability/aggressive tendencies in high school. Since onset, she had experienced auditory hallucinations and persecutory delusions, as well as continued irritability and aggression. Despite the efficacy of antipsychotic drugs on her positive symptoms, the patient suffered numerous relapses throughout her course of illness due to poor insight and lack of adherence to treatment. At the time of recruitment, she was 61 years old, with a chronic condition of diabetes and no comorbid mental conditions. She died in 2012 at the age of 62.

The patient carrying the *PTPRA* 174620_174623dupTGAT mutation was a male diagnosed with SCZ and comorbid intellectual disability at the age of 27, while he was enrolled in our study. He had a normal conception and birth, born to a 28-year-old father and 27-year-old mother. His father died when he was 3. Delayed intellectual development was observed since his childhood, with reports of illiteracy, hyperactivity, poor concentration and low performance at school. He subsequently dropped out of high school in his first year and started attending a technical school. After graduation, not being able maintain a steady position, he changed part-time jobs frequently. He presented at onset with hallucinations, persecutory delusions, and psychomotor excitement, and was subjected to involuntary commitment due to harmful behavior to others as a result of his delusions. At the time of admission, he was 168 cm tall and weighed 74 kg, with a Wechsler Adult Intelligence Scale (WAIS) score of 49 (Verbal IQ = 57, Performance IQ = 48); he also suffered from stuttering (anarthria literalis). After remission under antipsychotic treatment, he was discharged; however, lack of insight or compliance persisted. It was reported that his mother had a history of panic attacks, and one of his maternal relatives was also diagnosed with SCZ.

Discussion

To our knowledge, this is the first study that systematically screened all coding regions and 3′UTR of the *PTPRA* gene for rare variants in SCZ patients and assessed the association of identified mutations in such a study with SCZ/ASD.

Main Findings

In this study, we sequenced the encoding regions, splicing sites, and 3′UTR region of the *PTPRA* gene in 382 SCZ patients using the Sanger sequencing method, and discovered 8 rare variants. We then conducted association analysis in a much larger sample set for the 2 rare, missense mutations and one 3′UTR InDel identified during the mutation-screening phase in order to investigate their relationship with SCZ and/or ASD.

We were unable to detect a statistically significant association for any of the 3 mutations; this may be attributed partially to the low frequency of rare mutations in the population. However, according to our estimation using CaTS, the power calculator for two-stage association studies (http://www.sph.umich.edu/csg/abecasis/CaTS/), it would require a sample size of around 25,000 cases and controls for the study to obtain possible significance [39,40]. Also, L59P was only detected among SCZ patients in our sample, which infers possible connection of this mutation to the disorder. The evolutionary conservation status of the locus also indicates its biological importance.

Recent studies have discussed the limited impact of protein-coding variants detected in exome resequencing projects, attributing it partly to the fact that most associated variants alter gene expression rather than protein structure. These findings may help explain the lack of association for the 2 missense mutations we detected, while hinting that 174620_174623dupTGAT, predicted to be located within an expression-regulating element, may have a more significant effect. [10]

Additionally, an increasing amount of evidence suggests that genetic risks for SCZ and ASD may not be conferred by the effects of individual variants alone, but also the amplifying interactions between multiple susceptibility loci [41–44]. Thus it may be interesting to sequence the mutation carriers for additional related variants in future.

Limitations

Several limitations should be considered when interpreting the results of our study. The single candidate gene paradigm for a gene with less than robust ties to schizophrenia may have been one of the reasons leading to negative results. Besides, the Sanger method it employed predetermined its relatively small sample size and detection power in contrast with next generation resequencing. In addition, we did not have lymphoblastoid cell lines (LCLs) from the mutation carriers for expression analysis or blood samples from their family members for pedigree study. Therefore, we were unable to follow up the results with further biological evidence. Moreover, some potentially interesting regions of the *PTPRA* gene, such as the promoter, 5′UTR, and most of the intronic

Table 4. Evolutionary conservation information for rs61742029 and L59P

Mutation	Species	Match	Gene	AA	Alignment
L59P	Human	—	ENST00000380393	59	K T S N P T S S L T S *L S V A P T F S P N I T L
	Mutant	Not conserved	—	59	K T S N P T S S L T S *P S V A P T F S P N I T
	P. Troglodytes	All identical	ENSPTRG00000033879	59	K T S N P T S S L T S *L S V A P T F S P N I T
	M. Mulatta	All identical	ENSMMUG00000005878	59	K T S N P T S S L T S *L S V A P T F S P N I T
	F. Catus	All identical	ENSFCAG00000019232	59	K T S S P A S S V T S *L S V A P T F S P N L T
	M. Musculus	All identical	ENSMUSG00000027303	59	K T S N S T S S V I S *L S V A P T F S P N L T
	G. Gallus	All identical	ENSGALG00000015995	56	*L N V S - - - S P M T T
	T. Rubripes	All identical	ENSTRUG00000014770	99	P T P S P A S D G T L *L Q A D P N A T G R V L
	D.rerio	Not conserved	ENSDARG00000001769	101	P P V V P P P A V P I *P T V V L P V P P T P T
	D. Melanogaster	No homologue	—	N/A	
	C. Elegans	No alignment	C09D8.1	N/A	
	X. Tropicalis	All conserved	ENSXETG00000017982	71	T T A PF T T T R T A *V I L A P N V T D S I F
rs61742029	Human			664	L K K E E E C E S Y T *V R D L L V T N T R E N
	mutated	all conserved		664	S Y T * R D L L V T N T R E N
	Ptroglodytes	all identical	ENSPTRG00000033879	673	L K K E E E C E S Y T *V R D L L V T N T R E N
	Mmulatta	all identical	ENSMMUG00000005878	673	L K K E E E C E S Y T *V R D L L V T N T R E N
	Fcatus	all identical	ENSFCAG00000019232	674	L K K E E E C E S Y T *V R D L L V T N T R E N
	Mmusculus	all identical	ENSMUSG00000027303	700	L K K E E E C E S Y T *V R D L L V T N T R E N
	Ggallus	all identical	ENSGALG00000015995	680	L K K E E E C E S Y T *V R D L L V T N T R E N
	Trubripes	all identical	ENSTRUG00000014770	710	Y T *V R D L L V T N N R E N

*Marks the position of the amino acid change due to mutation.

doi:10.1371/journal.pone.0112531.t004